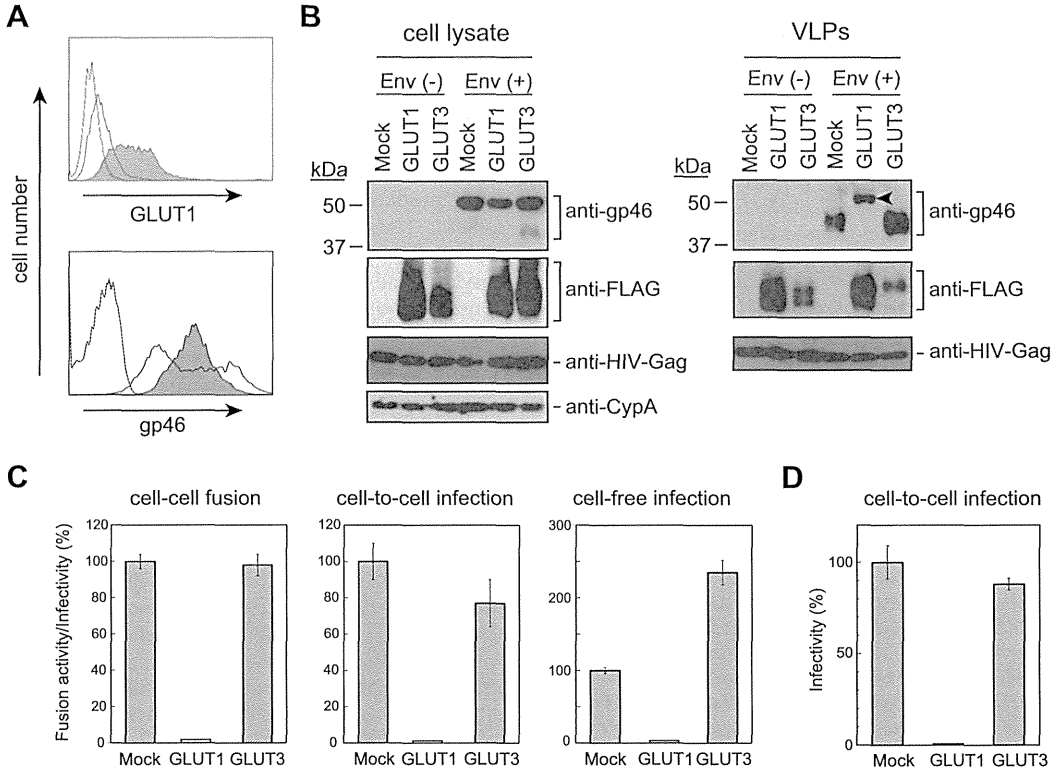

FIG 1 Effect of overexpression of GLUT1 in HTLV-1 Env-producing cells on HTLV-1 Env-mediated fusion and infection. (A) The HTLV-1 Env and FLAG-tagged GLUT1 were coexpressed in 293T cells and analyzed by flow cytometry. (Upper) Surface expression of GLUT1 in untransfected (open histograms with solid line) or FLAG-tagged-GLUT1-transfected (shaded histograms with solid line) cells. (Lower) Surface expression of gp46 in mock-cotransfected (transfected with HTLV-1 Env alone; open histogram with solid line) or FLAG-tagged GLUT1-cotransfected (transfected with both HTLV-1 Env and GLUT1; shaded histogram with solid line) cells. 293T cells were stained with FITC-conjugated anti-GLUT1 or anti-gp46 rat MAb, followed by anti-rat IgG conjugated with APC, and analyzed by flow cytometry. Open histograms with dotted lines indicate background staining. (B) Cell lysates and VLPs from 293T cells transfected with FLAG-tagged GLUT1 or GLUT3, with or without HTLV-1 Env, were analyzed by Western blotting using anti-FLAG, anti-gp46 (LAT-27), anti-HIV-Gag, and anti-CypA antibodies. The positions of the molecular mass marker (kDa) are indicated on the left. The arrowhead shows the ~53-kDa size of the Env protein. (C) HTLV-1 Env-carrying VLPs were produced using 293T cells cotransfected with FLAG-tagged GLUT1 or GLUT3. Relative cell-cell fusion activity, cell-to-cell infectivity, and cell-free virus infectivity of HTLV-1 Env in the presence of GLUT1 or GLUT3 in VLP-producing 293T cells are expressed as percentages of the level for mock-transfected 293T cells. (D) 293T cells were transfected with an HTLV-1 reporter construct for cell-to-cell infection (pCRU5-HTinGLucβ) and HTLV-1 packaging plasmids (pCMV-HT1M). Jurkat cells then were cocultured for 24 h posttransfection, and luciferase activity was measured after 48 h of coculture. Cell-to-cell infectivity of HTLV-1 Env in the presence of GLUT1 or GLUT3 in VLP-producing 293T cells is expressed as percentages of that of the level for mock-transfected 293T cells.

each chimera expressed in VLP-producing 293T cells was evaluated by a cell-cell fusion assay. We first confirmed that all chimeras were expressed at similar levels in 293T cells (Fig. 3B). The inhibition of the cell-cell fusion at levels similar to those induced by GLUT1 was observed in chimeras harboring extracellular loop 6 (ECL6) from GLUT1, though the GLUT1 (3-ECL6) chimera, which harbors GLUT1 with ECL6 from GLUT3, also had inhibitory activity against the cell-cell fusion to some extent. These results indicate that GLUT1 ECL6 is sufficient for the inhibition of cell fusion activity mediated by HTLV-1 Env.

Bafilomycin A1 inhibits HTLV-1 Env-mediated fusion by increasing the expression level of GLUT1 in the plasma membrane. It has been reported that an endosomal acidification inhibitor, bafilomycin A1 (BFLA1), which blocks vacuolar proton pump activity mediated by V-ATPase, induces the translocation of GLUT1 from intracellular storage sites to the plasma membranes in adipocytes (30). Flow-cytometric analyses revealed that the surface expression level of GLUT1 was increased by BFLA1 not only in GLUT1-trasnsfected cells but also in untransfected 293T cells (Fig. 4A), while the total levels of cellular GLUT1 were unchanged (Fig. 4B). These results indicate that BFLA1 induces the translocation of endogenous GLUT1 from intracellular storage sites to the plasma membrane in 293T cells. However, the surface expression level of gp46 was not affected by the treatment with BFLA1 (Fig. 4A).

The incorporation of GLUT1 in VLPs also was not affected by BFLA1 treatment (Fig. 4B). However, mature gp46 was not incorporated into VLPs in the presence of BFLA1, irrespective of the overexpression of GLUT1 or GLUT3 (Fig. 4B).

The cell-cell fusion, cell-to-cell infection, and cell-free infection mediated by HTLV-1 Env were totally inhibited by BFLA1 treatment (Fig. 4C) in 293T cells that were not overexpressing GLUT1. In contrast, when the target cells were treated with BFLA1, the cell-free virus infectivity was reduced to a lower rate than the rate observed when using virus from BFLA1-treated virus-infected cells (Fig. 4D), probably owing to the inhibition of HTLV-1 Env entry via the endocytic pathway (31). These results indicate that

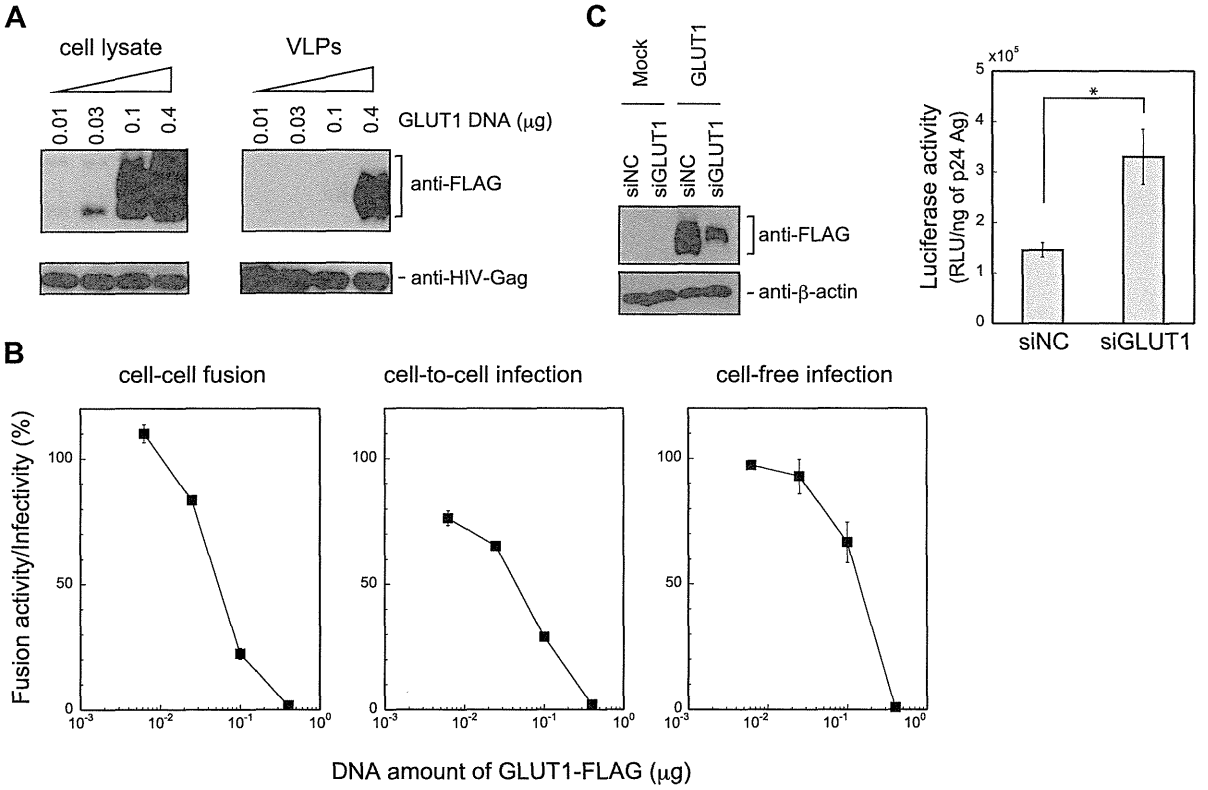

FIG 2 Dose-dependent effects of GLUT1 on HTLV-1 Env-mediated fusion and infection. (A) Cell lysates or VLPs from 293T cells transfected with increasing amounts of FLAG-tagged GLUT1 were analyzed by Western blotting using anti-FLAG and anti-HIV-Gag MAb. (B) Relative cell-cell fusion activity, cell-to-cell infectivity, and cell-free virus infectivity in 293T cells cotransfected with various amounts of GLUT1 DNA are expressed as percentages of those transfected with empty vector. (C) Luciferase-reporter VLPs were produced in 293T cells cotransfected with GLUT1 and the negative-control siRNA (siNC) or siRNA against GLUT 1 (siGLUT1). (Left) Knockdown of GLUT1 by siRNA as determined by Western blotting using anti-FLAG MAb. β-Actin levels were used as the internal control. (Right) Cell-free virus infectivity produced from 293T cells transfected with siGLUT1 or siNC. Data are expressed as the luciferase activity of infected NP-2/CD4/CXCR4/CCR5 cells per 1 ng of p24 Ag. The data are expressed as means ± standard deviations from three independent experiments in triplicate. An asterisk indicates a statistically significant difference ($P < 0.05$).

BFLA1 inhibits HTLV-1 Env function by inducing the accumulation of GLUT1 in the plasma membrane, producing results similar to those observed during the overexpression of GLUT1.

Association of GLUT1 and gp46 in intracellular compartments by bafilomycin A1. Inhibition of HTLV-1 Env function by the translocation of GLUT1 to the plasma membrane suggests that under normal conditions, GLUT1 and HTLV-1 Env reside in separate intracellular compartments. To test this hypothesis, we coexpressed FLAG-tagged GLUT1 and HTLV-1 Env in 293T cells and checked whether anti-FLAG antibody immunoprecipitates gp46 of HTLV-1 Env. We found that FLAG-tagged GLUT1 was able to coimmunoprecipitate gp46 in untreated cells, and that BFLA1 treatment largely enhanced this association of GLUT1 with gp46 (Fig. 5A). We next sought to check whether GLUT1 is colocalized with gp46 in intracellular compartments using laser scanning confocal microscopy. When GFP-tagged GLUT1 and HTLV-1 Env were coexpressed in 293T cells, both were partly colocalized, while treatment with BFLA1 substantially induced colocalization of both in intracellular compartments (Fig. 5B). These results indicate that most of the GLUT1 and HTLV-1 Env are localized in separate intracellular compartments, resulting in marginal association between them under normal conditions.

Overexpression of GLUT1 and bafilomycin A1 treatment both inhibit HTLV-1 Env processing. As shown in Fig. 4B, when the cells overexpressed GLUT1 or were treated with BFLA1, mature gp46 was not incorporated into VLPs, suggesting that these conditions cause an impairment in the processing of Env. To access the processing of Env, we constructed an expression vector for HTLV-1 Env with a FLAG tag in the C-terminal end (Fig. 6A). Successful processing of HTLV-1 Env by a cellular enzyme(s) should result in a cleaved TM region of 21 kDa, while unsuccessful processing should result in an uncleaved size of ~53 kDa. We found that overexpression of GLUT1, but not overexpression of GLUT3, in 293T cells inhibited the processing of Env (Fig. 6B). We further observed that treatment of 293T cells with BFLA1 also inhibited the processing of Env irrespective of the overexpression of GLUT1 or GLUT3 (Fig. 6B). These results imply that the cleavage of Env precursor is inhibited by the association of Env with GLUT1 in intracellular compartments.

DISCUSSION

Because GLUT1 has been shown to directly associate with gp46 of HTLV-1 Env as the receptor for HTLV-1 (32), we expected that a large amount of GLUT1 in virus-producing cells with HTLV-1

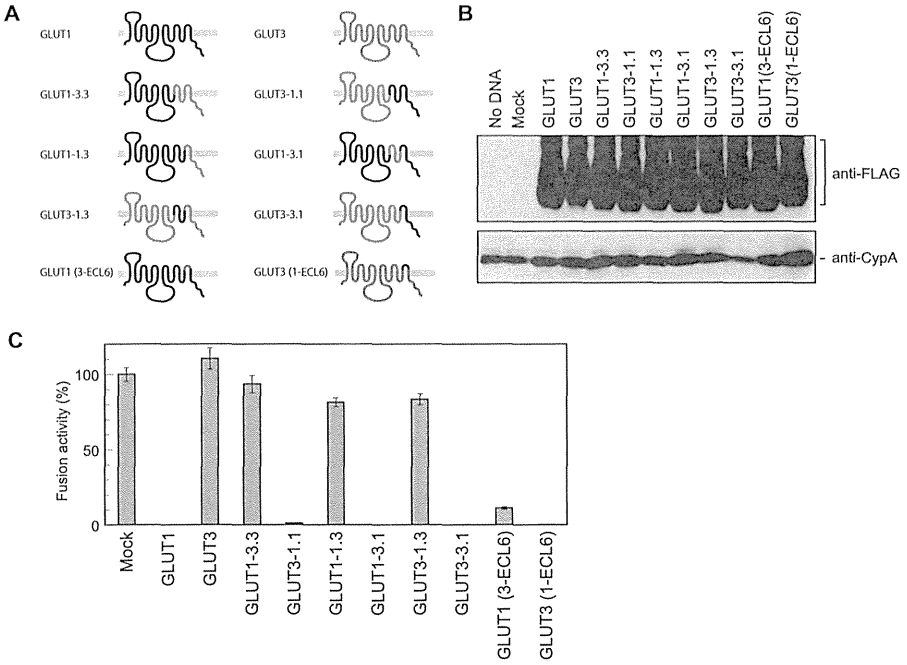

FIG 3 Determination of the region of GLUT1 responsible for the inhibitory activity against HTLV-1 Env-mediated fusion. (A) Schematic of chimeras between GLUT1 and GLUT3. (B) VLP-producing 293T cells were cotransfected with HTLV-1 Env and chimeras between GLUT1 and GLUT3. Cell lysates were analyzed by Western blotting using anti-FLAG MAb. CypA levels were used as the internal control. (C) Cell-cell fusion activity for each of the chimeras is expressed as the percentage of the level for empty vector.

Env would inhibit fusion activity and nascent progeny virus infectivity. Indeed, the overexpression of GLUT1 in VLP-producing cells impaired the HTLV-1 Env-mediated virus fusion and infection in a dose-dependent manner. Furthermore, a reduction of GLUT1 in virus-producing cells by an siRNA knockdown of endogenous GLUT1 enhanced the HTLV-1 Env-mediated infection. These results indicate that HTLV-1 Env-mediated fusion activity and infectivity are inversely correlated with the expression level of GLUT1 in cells productively infected with virus. Chimeric studies with GLUT3, which had no inhibitory activity against cell fusion and infection mediated by HTLV-1 Env, revealed that the ECL6 domain was crucial for the inhibitory activity of GLUT1. This domain previously has been shown to be sufficient for binding gp46, while other domains, such as ECL1 and ECL5, have some role(s) in the infection process (32). Taken together, GLUT1 in virus-infected cells should be regulated to low levels to avoid the interaction of HTLV-1 Env with GLUT1.

It has been shown that some of the enveloped viruses regulate their receptor(s) in virus-infected cells through their gene products. For example, to release the virus from the infected cells, influenza virus neuraminidase (NA) enzymatically cleaves sialic acids from sialic acid-containing receptors that are bound to the hemagglutinin (HA) (33–35). In the case of retroviruses, the downregulation of their receptors is believed to be necessary for preventing the infected cells from causing superinfection, which is known as superinfection interference (reviewed in reference 36). However, downregulation of the viral receptor also has been shown to maintain viral infectivity. Indeed, overexpression of CD4, which is the receptor for another human retrovirus, HIV-1, has been shown to impair the infectivity of HIV-1 (20, 37–39). To reduce the amount of CD4 in the infected cells, however, the HIV-1 accessory gene products, Nef and Vpu, induce downregulation and degradation, respectively, of the principal receptor CD4. Although HTLV-1 is a complex retrovirus that, like HIV-1, has several accessory genes, no HTLV-1 gene product has been shown to regulate its receptor molecules. In the present study, the overexpression of GLUT1 completely inhibited the HTLV-1 Env-mediated fusion and infection in VLPs made with HTLV-1 packaging plasmids, suggesting that HTLV-1 gene products do not involve the regulation of GLUT1, although this has not yet been fully confirmed.

It also has been reported that HIV-1 Nef downregulates its coreceptor, CCR5, in HIV-1-infected cells, although the effect was not as striking as the ability of Nef to downregulate CD4 (40, 41). We previously showed that the incorporation of larger amounts of HIV-1 coreceptor CCR5 into virions impaired the infectivity of HIV-1 when a CCR5-high $CD4^+$ T-cell line was infected with a distinct HIV-1 molecular clone, while a CCR5-low $CD4^+$ T-cell line was able to support virus infectivity (42). Because primary $CD4^+$ T cells express a low level of CCR5 in general (43, 44), the incorporation of CCR5 into virions and the interaction of CCR5 with HIV-1 gp120 are expected to be limited. Similarly, the incorporation of GLUT1 into VLPs was dependent on the expression level of GLUT1 in VLP-producing cells in the present study. Thus, it is likely that cells expressing a low level of GLUT1 should be selected as the target cells for HTLV-1 to produce nascent progeny virus.

It has been shown that $CD4^+$ and $CD8^+$ T cells, B cells, macrophages, myeloid cells, and fibroblasts have been infected with HTLV-1 (13, 45–48), which is not surprising, because GLUT1 is

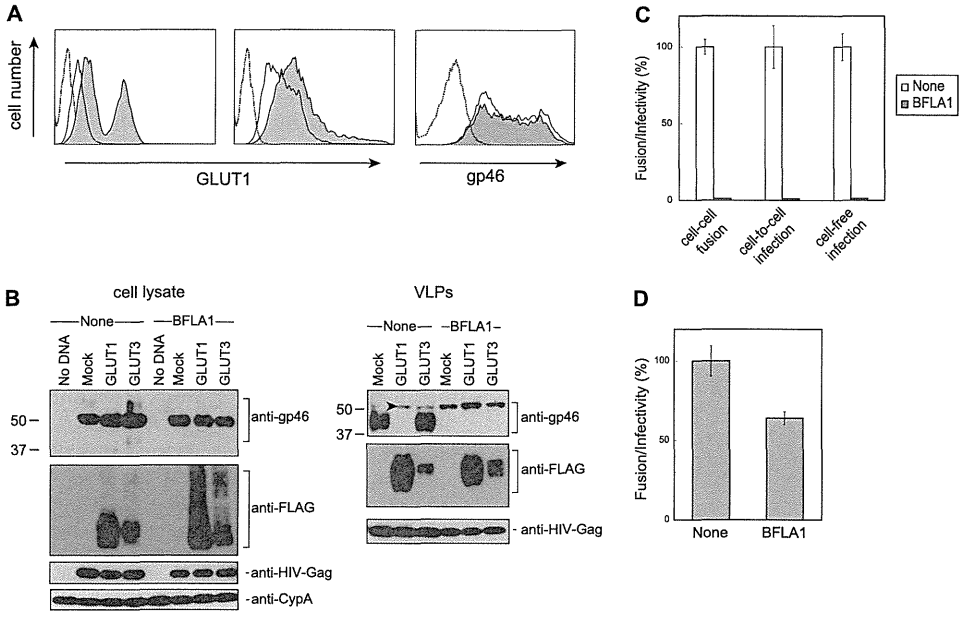

FIG 4 Effects of BFLA1 on the location of GLUT1 and on HTLV-1 Env-mediated fusion and infection. (A) Untransfected 293T cells (left) or 293T cells transfected with FLAG-tagged-GLUT1 and Env (middle and right) were cultured in the absence (open histograms with solid lines) or presence of 100 nM BFLA1 (shaded histograms with solid lines). The cells were stained with FITC-conjugated GLUT1 or anti-gp46 rat MAb (LAT-27), followed by anti-rat IgG conjugated with APC, and analyzed by flow cytometry. (Left and middle) Fluorescence intensity of GLUT1. (Right) Fluorescence intensity of gp46. Open histograms with dotted lines indicate background staining with secondary antibody alone. (B) Cell lysates and VLPs from 293T cells transfected with Env- and FLAG-tagged GLUT1 or GLUT3 in the absence or presence of BFLA1 were analyzed by Western blotting using anti-FLAG, anti-gp46 (LAT-27), anti-HIV-Gag, and anti-CypA antibodies. The positions of the molecular mass marker (in kDa) are indicated to the left. The arrowhead shows the ~53-kDa size of Env. (C) HTLV-1 Env-mediated fusion/infectivity was analyzed in the presence or absence of BFLA1. Relative fusion activity/infectivity in the presence of BFLA1 is expressed as the percentage of fusion/infectivity in the absence of BFLA1 (shown in the shaded bars). The data are expressed as means ± standard deviations from triplicate experiments. (D) 293T cells were transfected with HIV-1 reporter and HTLV-1 Env plasmids, and cell-free virus was recovered. Cell-free infectivity of HTLV-1 Env for NP-2/CD4/CXCR4/CCR5 cells in the presence of BFLA1 is expressed as the percentage of the infectivity for BFLA1-untreated NP-2/CD4/CXCR4/CCR5 cells.

ubiquitously expressed in these cells. It has been reported that $CD8^+$ T cells express much more GLUT1 than $CD4^+$ T cells (49, 50). Nonetheless, HTLV-1 is found primarily in $CD4^+$ T cells in infected individuals (15). The results from the present study suggest it is possible that $CD8^+$ T cells produce fusion-incompetent virus because of their higher expression of GLUT1. To efficiently use the small amount of GLUT1 in $CD4^+$ T cells for HTLV-1 entry, however, HTLV-1 may need to infect the cells via cell-to-cell contact.

Although our 293T cells endogenously express GLUT1 at low

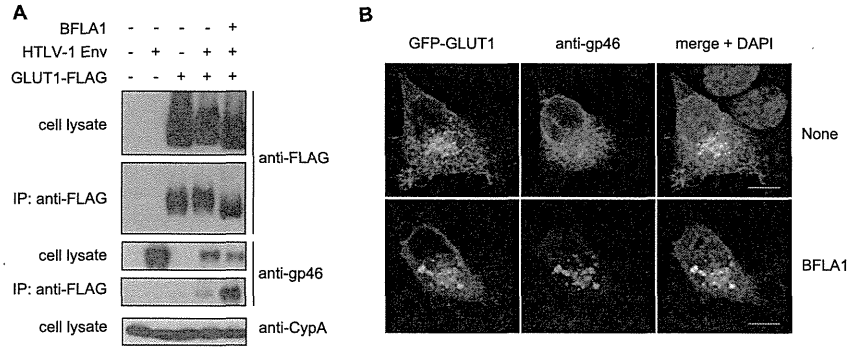

FIG 5 Effect of BFLA1 treatment on the association between GLUT1 and gp46 in intracellular compartments. (A) Lysates from 293T cells transfected with GLUT1-FLAG and HTLV-1 Env were analyzed by Western blotting using anti-FLAG, anti-gp46 (LAT-27), and anti-CypA antibodies. Immunoprecipitation (IP) was performed using anti-FLAG antibody with protein G-Sepharose beads, and blots were analyzed with anti-gp46 MAb. (B) HeLa cells were transiently transfected with plasmids encoding GFP-tagged GLUT1 and HTLV-1 Env and examined for localization of GLUT1 (green) and gp46 (red) 24 h posttransfection in the absence (upper) or presence (lower) of 100 nM BFLA1. Nuclei were counterstained with 4′,6-diamidino-2-phenylindole (DAPI) (blue). Scale bars correspond to 10 μm.

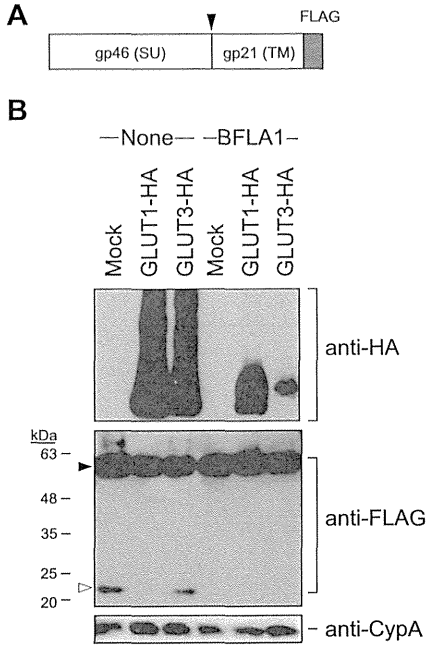

FIG 6 Effects of overexpression of GLUT1 or BFLA1 treatment on HTLV-1 Env processing. (A) Schematic of FLAG-tagged HTLV-1 Env. The arrowhead indicates the cleavage site of Env. (B) Cell lysates from 293T cells transfected with FLAG-tagged HTLV-1 Env and HA-tagged GLUT1 or GLUT3 were incubated in the presence or absence of BFLA1. Proteins were resolved with SDS-PAGE and immunoblotted with antibodies to HA, FLAG, and CypA. The positions of the molecular mass marker (kDa) are indicated to the left. The arrowheads at the left indicate positions of uncleaved Env (filled) and cleaved TM (hollow).

levels on their cell surfaces, similar to $CD4^+$ T cells, BFLA1 treatment enhanced the surface expression of endogenous GLUT1, while the total GLUT1 level was not affected (30). This result indicated that endogenous GLUT1 is localized mainly in intracellular compartments in 293T cells, although its exact location is unknown. In addition, BFLA1 treatment induced the enhanced binding of gp46 with GLUT1 and the colocalization of both molecules in the same intracellular compartments. Therefore, it is assumed that the overexpression of GLUT1 or translocation of endogenous GLUT1 into the plasma membrane induces the association of gp46 with GLUT1, thereby inhibiting the cell fusion and infection mediated by HTLV-1 Env.

When VLPs were produced in 293T cells expressed with larger amounts of GLUT1 or treated with BFLA1, mature gp46 was not incorporated into VLPs. FLAG-tagged HTLV-1 Env in VLP-producing cells confirmed that the precursor Env was not efficiently cleaved in GLUT1-overexpressed or BFLA1-treated 293T cells, probably owing to the direct association of Env with GLUT1. Previous studies have shown that the cleavage of retroviral Env is essential for the surface expression of Env, incorporation of Env into virions, and fusion activity of Env (51, 52). The lack of precursor Env cleavage of HTLV-1 Env by several experimental conditions, such as the treatment of cells with various inhibitors, also has been shown to reduce the surface expression of Env, leading to the loss of fusion activity (53). In our case, we showed that GLUT1-associated HTLV-1 Env was translocated to the cell surface, but mature gp46 was not incorporated into VLPs from GLUT1-overexpressed or BFLA1-treated 293T cells. These results indicate that trafficking of HTLV-1 Env occurs in spite of its association with GLUT1, but in cells with overexpressed GLUT1 or cells treated with BFLA-1 the conformational maturation of Env is impaired.

It should be noted that colocalization of GLUT1 with gp46 was partly observed in untreated 293T cells, while BFLA1 treatment enhanced the colocalization of both molecules not only in the plasma membrane but also in the cytoplasm. These results indicate that GLUT1 localizes in different intracellular compartments from gp46 under normal conditions. Because the processing of Env was inhibited by the association of Env with GLUT1, this association likely occurs in specific intracellular compartments, presumably in the endoplasmic reticulum or Golgi apparatus, though the exact location is not known. Although GLUT1 is thought to be an unregulated transporter responsible for the basal uptake of glucose in general, recycling between intracellular storage sites and the cell surface has been reported not only in adipocytes following BFLA1 treatment (30) but also in T cells following CD28 stimulation (54, 55). However, regulatory T (Treg) cells, which are $CD4^+$ and thought to be the principal target of HTLV-1 (56–58), do not express large amounts of GLUT1 upon stimulation (59–61). Thus, GLUT1 likely is regulated in HTLV-1-infected cells, thereby supporting HTLV-1 virus infectivity.

In conclusion, our present study provides new insight into how HTLV-1 regulates its receptor molecule(s) in virus-infected cells. Regulation of the receptor molecules is achieved not only through the viral gene products but also by the spatial regulation of the receptor molecules in virus-infected cells. However, our findings should be confirmed using natural target cells for HTLV-1 infection, such as $CD4^+$ T cells. Additionally, it remains to be determined how other receptor molecules are regulated during productive infection in HTLV-1-infected cells, such as DSPG and NRP-1. Further studies are necessary to understand the underlying molecular mechanism(s) in the regulation of receptors for HTLV-1 in infected cells.

ACKNOWLEDGMENTS

We are grateful to David Derse and Gisela Heidecker for providing HTLV-1 and HIV-1 packaging and reporter plasmids for cell-to-cell infection experiments. We also thank Masao Matsuoka for providing pMT-2 and Kazuaki Monde, Yusuke Nakano, and Yuzhe Yuan for helpful discussions.

This work was supported by a grant in aid for scientific research from the Ministry of Health of Japan.

REFERENCES

1. Gessain A, Vernant JC, Maurs L, Barin F, Gout O, Calender A, De Thé G. 1985. Antibodies to human T-lymphotropic virus type-I in patients with tropical spastic paraparesis. Lancet 326:407–410. http://dx.doi.org/10.1016/S0140-6736(85)92734-5.
2. Osame M, Janssen R, Kubota H, Nishitani H, Igata A, Nagataki S, Mori M, Goto I, Shimabukuro H, Khabbaz R, et al. 1990. Nationwide survey of HTLV-I-associated myelopathy in Japan: association with blood transfusion. Ann Neurol 28:50–56. http://dx.doi.org/10.1002/ana.410280110.
3. Manel N, Kim FJ, Kinet S, Taylor N, Sitbon M, Battini JL. 2003. The ubiquitous glucose transporter GLUT-1 is a receptor for HTLV. Cell 115:449–459. http://dx.doi.org/10.1016/S0092-8674(03)00881-X.
4. Jones KS, Petrow-Sadowski C, Bertolette DC, Huang Y, Ruscetti FW. 2005. Heparan sulfate proteoglycans mediate attachment and entry of human T-cell leukemia virus type 1 virions into CD4+ T cells. J Virol 79:12692–12702. http://dx.doi.org/10.1128/JVI.79.20.12692-12702.2005.

5. Lambert S, Bouttier M, Vassy R, Seigneuret M, Petrow-Sadowski C, Janvier S, Heveker N, Ruscetti FW, Perret G, Jones KS, Pique C. 2009. HTLV-1 uses HSPG and neuropilin-1 for entry by molecular mimicry of VEGF165. Blood 113:5176–5185. http://dx.doi.org/10.1182/blood-2008-04-150342.
6. Mazurov D, Ilinskaya A, Heidecker G, Lloyd P, Derse D. 2010. Quantitative comparison of HTLV-1 and HIV-1 cell-to-cell infection with new replication dependent vectors. PLoS Pathog 6:e1000788. http://dx.doi.org/10.1371/journal.ppat.1000788.
7. Popovic M, Sarin PS, Robert-Gurroff M, Kalyanaraman VS, Mann D, Minowada J, Gallo RC. 1983. Isolation and transmission of human retrovirus (human T-cell leukemia virus). Science 219:856–859. http://dx.doi.org/10.1126/science.6600519.
8. Yamamoto N, Okada M, Koyanagi Y, Kannagi M, Hinuma Y. 1982. Transformation of human leukocytes by cocultivation with an adult T cell leukemia virus producer cell line. Science 217:737–739. http://dx.doi.org/10.1126/science.6980467.
9. Igakura T, Stinchcombe JC, Goon PK, Taylor GP, Weber JN, Griffiths GM, Tanaka Y, Osame M, Bangham CR. 2003. Spread of HTLV-I between lymphocytes by virus-induced polarization of the cytoskeleton. Science 299:1713–1716. http://dx.doi.org/10.1126/science.1080115.
10. Pais-Correia AM, Sachse M, Guadagnini S, Robbiati V, Lasserre R, Gessain A, Gout O, Alcover A, Thoulouze MI. 2010. Biofilm-like extracellular viral assemblies mediate HTLV-1 cell-to-cell transmission at virological synapses. Nat Med 16:83–89. http://dx.doi.org/10.1038/nm.2065.
11. Jones KS, Petrow-Sadowski C, Huang YK, Bertolette DC, Ruscetti FW. 2008. Cell-free HTLV-1 infects dendritic cells leading to transmission and transformation of CD4(+) T cells. Nat Med 14:429–436. http://dx.doi.org/10.1038/nm1745.
12. Goon PK, Igakura T, Hanon E, Mosley AJ, Barfield A, Barnard AL, Kaftantzi L, Tanaka Y, Taylor GP, Weber JN, Bangham CR. 2004. Human T cell lymphotropic virus type I (HTLV-I)-specific CD4+ T cells: immunodominance hierarchy and preferential infection with HTLV-I. J Immunol 172:1735–1743. http://dx.doi.org/10.4049/jimmunol.172.3.1735.
13. Hanon E, Asquith RE, Taylor GP, Tanaka Y, Weber JN, Bangham CR. 2000. High frequency of viral protein expression in human T cell lymphotropic virus type 1-infected peripheral blood mononuclear cells. AIDS Res Hum Retrovir 16:1711–1715. http://dx.doi.org/10.1089/08892220050193191.
14. Hanon E, Hall S, Taylor GP, Saito M, Davis R, Tanaka Y, Usuku K, Osame M, Weber JN, Bangham CR. 2000. Abundant tax protein expression in CD4+ T cells infected with human T-cell lymphotropic virus type I (HTLV-I) is prevented by cytotoxic T lymphocytes. Blood 95:1386–1392.
15. Richardson JH, Edwards AJ, Cruickshank JK, Rudge P, Dalgleish AG. 1990. In vivo cellular tropism of human T-cell leukemia virus type 1. J Virol 64:5682–5687.
16. Uchiyama T. 1997. Human T cell leukemia virus type I (HTLV-I) and human diseases. Annu Rev Immunol 15:15–37. http://dx.doi.org/10.1146/annurev.immunol.15.1.15.
17. Aiken C, Konner J, Landau NR, Lenburg ME, Trono D. 1994. Nef induces CD4 endocytosis: requirement for a critical dileucine motif in the membrane-proximal CD4 cytoplasmic domain. Cell 76:853–864. http://dx.doi.org/10.1016/0092-8674(94)90360-3.
18. Garcia JV, Miller AD. 1991. Serine phosphorylation-independent down-regulation of cell-surface CD4 by nef. Nature 350:508–511. http://dx.doi.org/10.1038/350508a0.
19. Rhee SS, Marsh JW. 1994. Human immunodeficiency virus type 1 Nef-induced down-modulation of CD4 is due to rapid internalization and degradation of surface CD4. J Virol 68:5156–5163.
20. Bour S, Schubert U, Strebel K. 1995. The human immunodeficiency virus type 1 Vpu protein specifically binds to the cytoplasmic domain of CD4: implications for the mechanism of degradation. J Virol 69:1510–1520.
21. Margottin F, Bour SP, Durand H, Selig L, Benichou S, Richard V, Thomas D, Strebel K, Benarous R. 1998. A novel human WD protein, h-beta TrCp, that interacts with HIV-1 Vpu connects CD4 to the ER degradation pathway through an F-box motif. Mol Cell 1:565–574. http://dx.doi.org/10.1016/S1097-2765(00)80056-8.
22. Schubert U, Anton LC, Bacik I, Cox JH, Bour S, Bennink JR, Orlowski M, Strebel K, Yewdell JW. 1998. CD4 glycoprotein degradation induced by human immunodeficiency virus type 1 Vpu protein requires the function of proteasomes and the ubiquitin-conjugating pathway. J Virol 72:2280–2288.
23. Jinno A, Shimizu N, Soda Y, Haraguchi Y, Kitamura T, Hoshino H. 1998. Identification of the chemokine receptor TER1/CCR8 expressed in brain-derived cells and T cells as a new coreceptor for HIV-1 infection. Biochem Biophys Res Commun 243:497–502. http://dx.doi.org/10.1006/bbrc.1998.8130.
24. Maeda Y, Terasawa H, Nakano Y, Monde K, Yusa K, Oka S, Takiguchi M, Harada S. 2014. V3-independent competitive resistance of a dual-X4 HIV-1 to the CXCR4 inhibitor AMD3100. PLoS One 9:e89515. http://dx.doi.org/10.1371/journal.pone.0089515.
25. Clarke MF, Gelmann EP, Reitz MS, Jr. 1983. Homology of human T-cell leukaemia virus envelope gene with class I HLA gene. Nature 305:60–62. http://dx.doi.org/10.1038/305060a0.
26. Foda M, Harada S, Maeda Y. 2001. Role of V3 independent domains on a dualtropic human immunodeficiency virus type 1 (HIV-1) envelope gp120 in CCR5 coreceptor utilization and viral infectivity. Microbiol Immunol 45:521–530. http://dx.doi.org/10.1111/j.1348-0421.2001.tb02653.x.
27. Maeda Y, Foda M, Matsushita S, Harada S. 2000. Involvement of both the V2 and V3 regions of the CCR5-tropic human immunodeficiency virus type 1 envelope in reduced sensitivity to macrophage inflammatory protein 1α. J Virol 74:1787–1793. http://dx.doi.org/10.1128/JVI.74.4.1787-1793.2000.
28. Tanaka Y, Zeng L, Shiraki H, Shida H, Tozawa H. 1991. Identification of a neutralization epitope on the envelope gp46 antigen of human T cell leukemia virus type I and induction of neutralizing antibody by peptide immunization. J Immunol 147:354–360.
29. Simon JH, Fouchier RA, Southerling TE, Guerra CB, Grant CK, Malim MH. 1997. The Vif and Gag proteins of human immunodeficiency virus type 1 colocalize in infected human T cells. J Virol 71:5259–5267.
30. Chinni SR, Shisheva A. 1999. Arrest of endosome acidification by bafilomycin A1 mimics insulin action on GLUT4 translocation in 3T3-L1 adipocytes. Biochem J 339(Part 3):599–606. http://dx.doi.org/10.1042/0264-6021:3390599.
31. Trejo SR, Ratner L. 2000. The HTLV receptor is a widely expressed protein. Virology 268:41–48. http://dx.doi.org/10.1006/viro.2000.0143.
32. Manel N, Battini JL, Sitbon M. 2005. Human T cell leukemia virus envelope binding and virus entry are mediated by distinct domains of the glucose transporter GLUT1. J Biol Chem 280:29025–29029. http://dx.doi.org/10.1074/jbc.M504549200.
33. Liu C, Eichelberger MC, Compans RW, Air GM. 1995. Influenza type A virus neuraminidase does not play a role in viral entry, replication, assembly, or budding. J Virol 69:1099–1106.
34. Palese P, Tobita K, Ueda M, Compans RW. 1974. Characterization of temperature sensitive influenza virus mutants defective in neuraminidase. Virology 61:397–410. http://dx.doi.org/10.1016/0042-6822(74)90276-1.
35. Shibata S, Yamamoto-Goshima F, Maeno K, Hanaichi T, Fujita Y, Nakajima K, Imai M, Komatsu T, Sugiura S. 1993. Characterization of a temperature-sensitive influenza B virus mutant defective in neuraminidase. J Virol 67:3264–3273.
36. Nethe M, Berkhout B, van der Kuyl A. 2005. Retroviral superinfection resistance. Retrovirology 2:52. http://dx.doi.org/10.1186/1742-4690-2-52.
37. Cortés MJ, Wong-Staal F, Lama J. 2002. Cell surface CD4 interferes with the infectivity of HIV-1 particles released from T cells. J Biol Chem 277:1770–1779. http://dx.doi.org/10.1074/jbc.M109807200.
38. Lama J, Mangasarian A, Trono D. 1999. Cell-surface expression of CD4 reduces HIV-1 infectivity by blocking Env incorporation in a Nef- and Vpu-inhibitable manner. Curr Biol 9:622–631. http://dx.doi.org/10.1016/S0960-9822(99)80284-X.
39. Marshall WL, Diamond DC, Kowalski MM, Finberg RW. 1992. High level of surface CD4 prevents stable human immunodeficiency virus infection of T-cell transfectants. J Virol 66:5492–5499.
40. Michel N, Allespach I, Venzke S, Fackler OT, Keppler OT. 2005. The Nef protein of human immunodeficiency virus establishes superinfection immunity by a dual strategy to downregulate cell-surface CCR5 and CD4. Curr Biol 15:714–723. http://dx.doi.org/10.1016/j.cub.2005.02.058.
41. Mwimanzi P, Hasan Z, Tokunaga M, Gatanaga H, Oka S, Ueno T. 2010. Naturally arising HIV-1 Nef variants conferring escape from cytotoxic T lymphocytes influence viral entry co-receptor expression and susceptibility to superinfection. Biochem Biophys Res Commun 403:422–427. http://dx.doi.org/10.1016/j.bbrc.2010.11.047.
42. Monde K, Maeda Y, Tanaka Y, Harada S, Yusa K. 2007. Gp120 V3-

dependent impairment of R5 HIV-1 infectivity due to virion-incorporated CCR5. J Biol Chem 282:36923–36932. http://dx.doi.org/10.1074/jbc.M705298200.
43. Moore JP. 1997. Coreceptors: implications for HIV pathogenesis and therapy. Science 276:51–52. http://dx.doi.org/10.1126/science.276.5309.51.
44. Wu L, Paxton WA, Kassam N, Ruffing N, Rottman JB, Sullivan N, Choe H, Sodroski J, Newman W, Koup RA, Mackay CR. 1997. CCR5 levels and expression pattern correlate with infectability by macrophage-tropic HIV-1, in vitro. J Exp Med 185:1681–1692. http://dx.doi.org/10.1084/jem.185.9.1681.
45. Eiraku N, Hingorani R, Ijichi S, Machigashira K, Gregersen PK, Monteiro J, Usuku K, Yashiki S, Sonoda S, Osame M, Hall WW. 1998. Clonal expansion within CD4+ and CD8+ T cell subsets in human T lymphotropic virus type I-infected individuals. J Immunol 161:6674–6680.
46. Grant C, Barmak K, Alefantis T, Yao J, Jacobson S, Wigdahl B. 2002. Human T cell leukemia virus type I and neurologic disease: events in bone marrow, peripheral blood, and central nervous system during normal immune surveillance and neuroinflammation. J Cell Physiol 190:133–159. http://dx.doi.org/10.1002/jcp.10053.
47. Nagai M, Brennan MB, Sakai JA, Mora CA, Jacobson S. 2001. CD8+ T cells are an in vivo reservoir for human T-cell lymphotropic virus type I. Blood 98:1858–1861. http://dx.doi.org/10.1182/blood.V98.6.1858.
48. Walter MJ, Lehky TJ, Fox CH, Jacobson S. 1994. In situ PCR for the detection of HTLV-I in HAM/TSP patients. Ann N Y Acad Sci 724:404–413. http://dx.doi.org/10.1111/j.1749-6632.1994.tb38939.x.
49. Jones KS, Fugo K, Petrow-Sadowski C, Huang Y, Bertolette DC, Lisinski I, Cushman SW, Jacobson S, Ruscetti FW. 2006. Human T-cell leukemia virus type 1 (HTLV-1) and HTLV-2 use different receptor complexes to enter T cells. J Virol 80:8291–8302. http://dx.doi.org/10.1128/JVI.00389-06.
50. Takenouchi N, Jones KS, Lisinski I, Fugo K, Yao K, Cushman SW, Ruscetti FW, Jacobson S. 2007. GLUT1 is not the primary binding receptor but is associated with cell-to-cell transmission of human T-cell leukemia virus type 1. J Virol 81:1506–1510. http://dx.doi.org/10.1128/JVI.01522-06.
51. McCune JM, Rabin LB, Feinberg MB, Lieberman M, Kosek JC, Reyes GR, Weissman IL. 1988. Endoproteolytic cleavage of gp160 is required for the activation of human immunodeficiency virus. Cell 53:55–67. http://dx.doi.org/10.1016/0092-8674(88)90487-4.
52. Perez LG, Hunter E. 1987. Mutations within the proteolytic cleavage site of the Rous sarcoma virus glycoprotein that block processing to gp85 and gp37. J Virol 61:1609–1614.
53. Pique C, Pham D, Tursz T, Dokhélar MC. 1992. Human T-cell leukemia virus type I envelope protein maturation process: requirements for syncytium formation. J Virol 66:906–913.
54. Jacobs SR, Herman CE, MacIver NJ, Wofford JA, Wieman HL, Hammen JJ, Rathmell JC. 2008. Glucose uptake is limiting in T cell activation and requires CD28-mediated Akt-dependent and independent pathways. J Immunol 180:4476–4486. http://dx.doi.org/10.4049/jimmunol.180.7.4476.
55. MacIver NJ, Jacobs SR, Wieman HL, Wofford JA, Coloff JL, Rathmell JC. 2008. Glucose metabolism in lymphocytes is a regulated process with significant effects on immune cell function and survival. J Leukoc Biol 84:949–957. http://dx.doi.org/10.1189/jlb.0108024.
56. Karube K, Ohshima K, Tsuchiya T, Yamaguchi T, Kawano R, Suzumiya J, Utsunomiya A, Harada M, Kikuchi M. 2004. Expression of FoxP3, a key molecule in CD4+CD25+ regulatory T cells, in adult T-cell leukaemia/lymphoma cells. Br J Haematol 126:81–84. http://dx.doi.org/10.1111/j.1365-2141.2004.04999.x.
57. Satou Y, Utsunomiya A, Tanabe J, Nakagawa M, Nosaka K, Matsuoka M. 2012. HTLV-1 modulates the frequency and phenotype of FoxP3+CD4+ T cells in virus-infected individuals. Retrovirology 9:46. http://dx.doi.org/10.1186/1742-4690-9-46.
58. Toulza F, Heaps A, Tanaka Y, Taylor GP, Bangham CRM. 2008. High frequency of CD4+FoxP3+ cells in HTLV-1 infection: inverse correlation with HTLV-1-specific CTL response. Blood 111:5047–5053. http://dx.doi.org/10.1182/blood-2007-10-118539.
59. Macintyre AN, Gerriets VA, Nichols AG, Michalek RD, Rudolph MC, Deoliveira D, Anderson SM, Abel ED, Chen BJ, Hale LP, Rathmell JC. 2014. The glucose transporter Glut1 is selectively essential for CD4 T cell activation and effector function. Cell Metab 20:61–72. http://dx.doi.org/10.1016/j.cmet.2014.05.004.
60. Michalek RD, Gerriets VA, Jacobs SR, Macintyre AN, MacIver NJ, Mason EF, Sullivan SA, Nichols AG, Rathmell JC. 2011. Cutting edge: distinct glycolytic and lipid oxidative metabolic programs are essential for effector and regulatory CD4+ T cell subsets. J Immunol 186:3299–3303. http://dx.doi.org/10.4049/jimmunol.1003613.
61. Michalek RD, Gerriets VA, Nichols AG, Inoue M, Kazmin D, Chang C-Y, Dwyer MA, Nelson ER, Pollizzi KN, Ilkayeva O, Giguere V, Zuercher WJ, Powell JD, Shinohara ML, McDonnell DP, Rathmell JC. 2011. Estrogen-related receptor-α is a metabolic regulator of effector T-cell activation and differentiation. Proc Natl Acad Sci U S A 108:18348–18353. http://dx.doi.org/10.1073/pnas.1108856108.
62. Hinuma Y, Nagata K, Hanaoka M, Nakai M, Matsumoto T, Kinoshita KI, Shirakawa S, Miyoshi I. 1981. Adult T-cell leukemia: antigen in an ATL cell line and detection of antibodies to the antigen in human sera. Proc Natl Acad Sci U S A 78:6476–6480. http://dx.doi.org/10.1073/pnas.78.10.6476.
63. Takatsuki K. 2005. Discovery of adult T-cell leukemia. Retrovirology 2:16. http://dx.doi.org/10.1186/1742-4690-2-16.
64. Yoshida M, Miyoshi I, Hinuma Y. 1982. Isolation and characterization of retrovirus from cell lines of human adult T-cell leukemia and its implication in the disease. Proc Natl Acad Sci U S A 79:2031–2035. http://dx.doi.org/10.1073/pnas.79.6.2031.

Transplant Infectious Disease, ISSN 1398-2273

Letter to the Editor

Nine-year follow-up in a child with chromosomal integration of human herpesvirus 6 transmitted from an unrelated donor through the Japan Marrow Donor Program

H. Yagasaki, H. Shichino, N. Shimizu, T. Ohye, H. Kurahashi, T. Yoshikawa, S. Takahashi. Nine-year follow-up in a child with chromosomal integration of human herpesvirus 6 transmitted from an unrelated donor through the Japan Marrow Donor Program. Transpl Infect Dis 2015: **17**: 160–161. All rights reserved

H. Yagasaki[1], H. Shichino[1], N. Shimizu[2], T. Ohye[3], H. Kurahashi[3], T. Yoshikawa[4], S. Takahashi[1]

[1]Pediatrics, School of Medicine, Nihon University, Tokyo, Japan, [2]Department of Virology, Medical Research Institute, Tokyo Medical and Dental University, Tokyo, Japan, [3]Division of Molecular Genetics, Institute for Comprehensive Medical Science, Fujita Health University, Aichi, Japan, [4]Pediatrics, School of Medicine, Fujita Health University, Aichi, Japan

Key words: human herpesvirus 6; transplantation; chomosomal integration

Correspondence to:
Dr Hiroshi Yagasaki, Pediatrics, Nihon University, 30-1 Ohyaguchi, Itabashi-ku, Tokyo 173-8610, Japan
Tel: +81-3-3972-8111
Fax: +81-3-3957-6186
E-mail: yagasaki.hiroshi@nihon-u.ac.jp

Received 20 November 2014, accepted for publication 4 December 2014

DOI: 10.1111/tid.12338
Transpl Infect Dis 2015: **17:** 160–161

To the Editor

Since 1993, several investigators have reported a unique phenomenon of chromosomal integration of human herpesvirus 6 (CIHHV-6), in which HHV-6 genome is randomly integrated into a human chromosome and vertically transmitted (1, 2). In Japan, the frequency of CIHHV-6 in healthy volunteers is 0.21% (3). CIHHV-6 has also been found in patients who have received hematopoietic stem cell transplantation (SCT), including cord blood transplantation (4–6). CIHHV-6 is generally believed to be innocuous for such a recipient.

Here, we present a patient in whom CIHHV-6 was transmitted from unrelated donor marrow transplantation (UR-BMT) through the Japan Marrow Donor Program. This study was performed according to the Helsinki declaration and informed consent was obtained from the patient's guardians. A fluorescence *in situ* hybridization (FISH) study was approved by the Ethical Review Board for Human Genome Studies at Fujita Health University.

The patient was a 15-year-old girl. She presented with severe anemia with pure red cell aplasia of the bone marrow. She was diagnosed with Diamond-Blackfan anemia soon after birth. She received UR-BMT at the age of 10 years, and obtained complete donor type engraftment. At the age of 15 years, she was admitted with severe pancreatitis and hepatitis

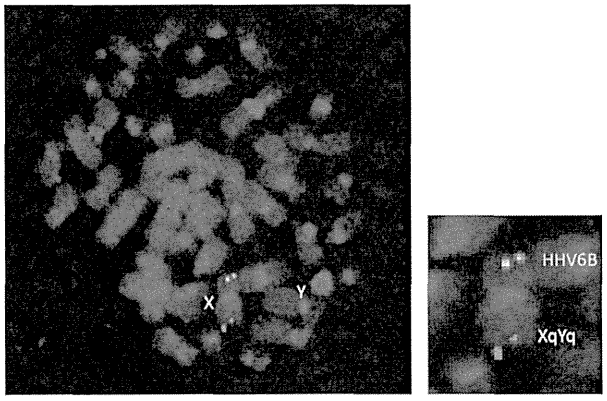

Fig. 1. Human herpevirus-6B (HHV6B) integrated into the chromosome Xp. Green signals and red signals showed HHV-6B and Xq/Yq sequence, respectively. Because the Y chromosome was also stained, this chromosome was proved to be of donor origin.

after endoscopic treatment for gallstones. She received cyclosporine for chronic graft-versus-host disease of the skin; therefore, we screened for infection with herpes simplex virus (HSV)-1, HSV-2, varicella zoster virus, Epstein–Barr virus, cytomegalovirus, HHV-6, HHV-7, JC virus, BK virus, and parvovirus by polymerase chain reaction. Surprisingly, we found a high copy number of HHV-6 (1.1×10^7 copies/μg DNA) in the peripheral blood. We began foscarnet treatment in addition to supportive care.

Although her general status improved rapidly, the HHV-6 genome load increased to 1.3×10^7 copies/μg DNA at day 38 after admission. At this time, we suspected CIHHV-6 phenomenon and measured HHV-6 genome load of her own cryopreserved blood before UR-BMT, and the donor's cryopreserved marrow sample at transplantation. As a result, HHV-6 genome was high (1.25×10^7 copies/μg DNA) in the donor's but not in the recipient's sample. FISH confirmed integration of HHV-6B genome into the donor's chromosome Xp subtelomeric region (Fig. 1) (7).

At present, she is 19 years old and well. Normal hematopoiesis is sustained as follows: white blood cell count 6100/μL (neutrophils 61%, lymphocytes 28%, monocytes 5%, eosinophils 5%, and basophils 1%), hemoglobin 13.9 g/dL reticulocytes 19%, and platelet count 30.8×10^4/μL. Other infectious events have not been observed during this period.

Although this episode suggests that CIHHV-6 is a silent bystander, the clinical significance of CIHHV-6 is not yet determined (6, 8). Recently, HHV-6 activation from CIHHV-6 was demonstrated in a boy with severe combined immunodeficiency (9). Another important issue is the long-term data in SCT recipients, which are lacking. The follow-up duration of 9 years in this report is the longest observation time among similar cases, to our knowledge.

HHV-6 genome load in both donor and recipient should be checked before any type of transplantation, as proposed by other investigators (8, 9). A nationwide survey is needed in such recipients.

Acknowledgements:

Author contributions: H.Y. designed the research and wrote the letter; T.O. and N.S. performed FISH and viral tests, respectively; H.S. analyzed the data; H.K. and T.Y. reviewed the draft critically. S.T. supervised the study.

Conflicts: None of the authors have any financial interests to declare.

References

1. Luppi M, Marasca R, Barozzi P, et al. Three cases of human herpesvirus-6 latent infection: integration of viral genome in peripheral blood mononuclear cell DNA. J Med Virol 1993; 40: 44–52.
2. Daibata M, Taguchi T, Nemoto Y, Taguchi H, Miyoshi I. Inheritance of chromosomally integrated human herpesvirus 6 DNA. Blood 1999; 94: 1545–1549.
3. Tanaka-Taya K, Sashihara J, Kurahashi H, et al. Human herpesvirus 6 (HHV-6) is transmitted from parent to child in an integrated form and characterization of cases with chromosomally integrated HHV-6 DNA. J Med Virol 2004; 73: 465–473.
4. Mori T, Tanaka-Taya K, Satoh H, et al. Transmission of chromosomally integrated human herpesvirus 6 (HHV-6) variant A from a parent to children leading to misdiagnosis of active HHV-6 infection. Transpl Infect Dis 2009; 11 (6): 503–506.
5. de Pagter PJ, Virgili A, Nacheva E, van Baarle D, Schuurman R, Boelens JJ. Chromosomally integrated human herpesvirus 6: transmission via cord blood derived unrelated hematopietic stem cell transplantation. Biol Blood Marrow Transplant 2010; 16: 130–132.
6. Pellett PE, Ablashi DV, Ambros PF, et al. Chromosomally integrated human herpesvirus 6: questions and answers. Rev Med Virol 2012; 22: 144–155.
7. Ohye T, Inagaki H, Ihira M, et al. Dual roles for the telomeric repeats in chromosomally integrated human herpesvirus-6. Sci Rep 2014; 4: 4559.
8. Morissette G, Flamand L. Herpesviruses and chromosomal integration. J Virol 2010; 84: 12100–12109.
9. Endo A, Watanabe K, Ohye T, et al. Molecular and virological evidence of viral activation from chromosomally integrated human herpesvirus 6A in a patient with X-linked severe combined immunodeficiency. Clin Infect Dis 2014; 59: 545–548.

Leukemia & Lymphoma, 2014; Early Online: 1–8

ISSN: 1042-8194 print / 1029-2403 online
DOI: 10.3109/10428194.2014.983099

informa
healthcare

ORIGINAL ARTICLE: CLINICAL

Epstein–Barr virus-associated T/natural killer-cell lymphoproliferative disorder in children and young adults has similar molecular signature to extranodal nasal natural killer/T-cell lymphoma but shows distinctive stem cell-like phenotype

Siok-Bian Ng[1,2,3], Koichi Ohshima[4], Viknesvaran Selvarajan[1], Gaofeng Huang[3], Shoa-Nian Choo[1], Hiroaki Miyoshi[4], Norio Shimizu[5], Renji Reghunathan[3], Hsin-Chieh Chua[6], Allen Eng-Juh Yeoh[6], Thuan-Chong Quah[6], Liang-Piu Koh[7], Poh-Lin Tan[6] & Wee-Joo Chng[2,3,7]

[1]*Department of Pathology and* [7]*Department of Haematology-Oncology, National University Cancer Institute of Singapore, National University Health System, Singapore,* [2]*Yong Loo Lin School of Medicine and* [3]*Cancer Science Institute of Singapore, National University of Singapore, Singapore,* [4]*Department of Pathology, Kurume University, Kurume, Japan,* [5]*Department of Virology, Tokyo Medical and Dental University, Tokyo, Japan and* [6]*Department of Pediatrics, National University Health System, Singapore*

Abstract

We performed gene expression profiling in Epstein–Barr virus (EBV)-associated T/natural killer (NK)-cell lymphoproliferative disorder in children and young adults (TNKLPDC) in order to understand the molecular pathways deregulated in this disease and compared it with nasal-type NK/T-cell lymphoma (NKTL). The molecular and phenotypic signature of TNKLPDC is similar to NKTL, with overexpression of p53, survivin and EZH2. Down-regulation of EZH2 in TNKLPDC cell lines led to an increase in apoptosis and decrease in tumor viability, suggesting that EZH2 may be important for the survival of TNKLPDC cells and hence potentially a useful therapeutic target. Notably, our gene expression profiling revealed a distinctive enrichment of stem cell related genes in TNKLPDC compared to NKTL. This was validated by a significantly higher expression of aldehyde dehydrogenase 1 (ALDH1) in TNKLPDC cell lines compared to NKTL cell lines. The novel discovery of cancer stem cell properties in TNKLPDC has potential therapeutic implications in this group of disorders.

Keywords: EBV+ T/NKLPD in children, molecular signature, cancer stem cell, EZH2

Introduction

Chronic active Epstein–Barr virus (EBV) infection of T/natural killer (NK)-cell type (CAEBV-T/NK) and systemic EBV-positive T-cell lymphoproliferative disease of childhood (STLPDC) are a group of diseases characterized by a systemic EBV-infected, cytotoxic T or NK cell proliferation [1,2]. According to the 2008 World Health Organization (WHO) classification, STLPDC is defined as a monoclonal disease of EBV-infected T-cells while CAEBV is polyclonal [1]. Since these entities show similar and overlapping clinicopathologic features, they have now been collectively referred to as EBV-associated T/NK lymphoproliferative disorders of childhood and young adults (TNKLPDC) (or EBV-associated T/NK lymphoproliferative disorders in non-immunocompromised hosts) [3–7]. Like many EBV-related T/NK lymphoproliferative diseases, TNKLPDC is prevalent in children and young adults in East Asia, Central and South America and Mexico [1,2].

The precise distinction of TNKLPDC from other EBV-associated T/NK lymphomas occurring in adults, such as nasal-type NK/T cell lymphoma (NKTL), can be notoriously difficult because of significant clinicopathologic overlap. Although classically a disease of childhood and young adults, increasing reports of TNKLPDC in adults have been documented, which may reflect a true increase in adult-onset disease or improved recognition and diagnosis of the disease [5,8,9]. In addition, even though CAEBV is a chronic disease and patients with clonal expansion of EBV-infected T and NK cells may remain stable for years without treatment, a proportion of patients with CAEBV will progress to aggressive lymphomas such as aggressive NK cell leukemia (ANKL) and NKTL [8,9]. Isobe *et al.* recently described seven cases of adult onset CAEBV, which shares common features with pediatric cases but with a poor prognosis, and five of seven patients developed T/NK cell lymphomas and ANKL at a

Correspondence: Siok-Bian Ng, Associate Professor, Department of Pathology, National University Hospital, 5 Lower Kent Ridge Road, Main Building, Level 3, Singapore 119074. Tel: 65-67724709. Fax: 65-67780671. E-mail: patnsb@nus.edu.sgmailto, siok_bian_ng@nuhs.edu.sg. Wee-Joo Chng, Associate Professor, Department of Hematology-Oncology, National University Cancer Institute of Singapore, National University Health System (NUHS), 1E, Kent Ridge Rd, Singapore 119228. Tel: 65-67724612, Fax: 65-67775545. E-mail: mdccwj@nus.edu.sg

Received 23 September 2014; accepted 13 October 2014

median of 5 years [9]. Furthermore, patients with NKTL can also present with disseminated disease that becomes indistinguishable from TNKLPDC.

The molecular abnormalities underlying TNKLPDC and its relationship with NKTL are poorly characterized because TNKLPDC is uncommon, and research on this entity is challenging as most of the tissue biopsies are bone marrow biopsies containing a limited amount of tumor. In this study, we performed, for the first time, gene expression profiling (GEP) on TNKLPDC and compared the signature with that of NKTL obtained in our previous study [10], with the objective of understanding the molecular pathways deregulated in this disease and to determine whether the molecular signature of TNKLPDC is distinct from NKTL.

Methods

Case selection

Patients with a diagnosis of EBV-associated T/NK-cell lymphoproliferative disorder without known underlying immune deficiency were identified from the archives of the Department of Pathology, National University Hospital (NUH) and Kurume University, from 2003 to 2014. Cases were classified according to the 2008 WHO lymphoma classification and nomenclature proposed following the National Institutes of Health (NIH) consensus report in 2008 [3]. A total of 22 cases of TNKLPDC with adequate material for work-up and fulfilling the diagnostic criteria were identified. The 22 cases included three cases of chronic active EBV infection of T/NK type (CAEBV), 15 cases of systemic EBV-associated T-cell LPD of childhood (STLPDC) and four cases with features borderline between CAEBV and STLPDC. We considered the presence of an abnormal karyotype and/or monoclonal TCRG gene rearrangement as indicative of a clonal proliferation [2]. The four cases were difficult to classify accurately because of lack of clonality data, which distinguish between CAEBV (polyclonal) and STLPDC (monoclonal) as defined by the WHO [1]. The clinicopathological features of the cases are included in Supplementary Table I to be found online at http://informahealthcare.com/doi/abs/10.3109/10428194.2014.983099. Cases of extranodal nasal type NKTL were excluded. Four cases of TNKLPDC with adequate formalin-fixed paraffin-embedded (FFPE) tissue and good quality RNA were selected for GEP (cases 5, 7, 16, 17). FFPE control tissues from normal skin and lymph nodes were included. This study was approved by the Domain Specific Review Board of the National Healthcare Group, Singapore.

Gene expression profiling and analysis

Total RNA from human FFPE tissues was isolated using a High Pure RNA Paraffin Kit (Roche Applied Science, Mannheim, Germany). We conducted genome-wide GEP on TNKLPDC and normal control FFPE samples using an Illumina WG-DASL Assay (Whole Genome cDNA-mediated Annealing, Selection, and Ligation) (Illumina, Inc., San Diego, CA) [11,12]. Raw signals are extracted from Illumina Beadstudio software, and normalized using a linear calibration method, as we have previously described [10]. Analysis of the data was done by R/Bioconductor.

In order to determine the similarity in GEP between NKTL and TNKLPDC, we calculated the expression fold-change for each gene as the mean expression of the gene in TNKLPDC samples and mean expression in normal samples. We plotted this fold-change between TNKLPDC and normal versus the fold-change between NKTL and normal (obtained from our previous study) [10] to determine the degree of Pearson correlation. To determine the genes specific to TNKLPDC in comparison to NKTL and normal tissues, we first selected genes with more than two-fold change between TNKLPDC and normal tissues, which constituted the candidate list of differentially expressed genes in TNKLPDC. Then using significance analysis of microarrays (SAM) [13] we generated another list of genes that was abnormally expressed between TNKLPDC and NKTL, with *cut-off* fold-change > 2 and p-value < 0.01. The intersection of the above two lists resulted in a final list of genes that were abnormally expressed specifically in TNKLPDC compared to NKTL and normal tissues.

Immunohistochemistry

In order to validate the expression of p53, survivin and EZH2 in the tumor and not the non-neoplastic population, we performed the following double stains: CD3/p53, CD3/survivin and CD3/EZH2, on 4 µm tissue sections of TNKLPDC samples using a Leica BondMax auto-stainer, and conditions are listed in Supplementary Table II to be found online at http://informahealthcare.com/doi/abs/10.3109/10428194.2014.983099. Appropriate positive tissue controls were used. The immunohistochemical (IHC) expression of all the antibodies was scored as a percentage of the tumor cell population by one of the authors (S.-B.N.), without knowledge of the clinicopathologic and GEP data. For p53 and survivin antibodies, positive expression was defined as nuclear staining in 10% or more of the tumor population, as previously described [10]. For EZH2 antibody, positive expression was defined as nuclear staining in 25% or more of the tumor population, as previously described [14].

TNKLPDC and NKTL cell line culture for ALDH analysis and DZNep treatment

Six NKTL cell lines (NK-92, HANK-1, NK-YS, SNK-1, SNK-6, SNT-8) and five TNKLPDC cell lines (KAI-3, SNK-10, SNT-13, SNT-15, SNT-16) were used in this study. NK-92 was purchased from the American Type Culture Collection (ATCC). HANK-1 was obtained as a kind gift from Dr. Y. Kagami, NK-YS and KAI-3 were from Dr. Y. L. Kwong while SNK-1, SNK-6, SNT-8, SNK-10, SNT-13, SNT-15 and SNT-16 were from Dr. N. Shimizu. Please refer to Supplementary Table III to be found online at http://informahealthcare.com/doi/abs/10.3109/10428194.2014.983099 for cell line culture conditions and Supplementary Table IV to be found online at http://informahealthcare.com/doi/abs/10.3109/10428194.2014.983099 for clinical, phenotypic and genotypic features of the TNKLPDC and NKTL cell lines.

ALDH analysis on NKTL and TNKLPDC cell lines

An ALDEFLUOR kit (Stem Cell Technologies, Durham, NC) was used to examine the aldehyde dehydrogenase

(ALDH) enzymatic activity in NKTL and TNKLPDC cell lines. A single cell suspension was prepared in ALDEFLUOR assay buffer containing ALDH substrate. As negative controls, each sample was treated with diethylaminobenzaldehyde (DEAB), a specific ALDH inhibitor. This resulted in a significant decrease in the fluorescence intensity of ALDH+ cells and was used to identify ALDH+ cells. The amount of intracellular fluorescence was measured using a BD LSR II (Becton Dickinson, San Diego, CA) flow cytometer and analyzed using BD FACSDiva™ software.

Treatment of TNKLPDC cell lines with DZNep

Exponentially growing cells of KAI-3, SNK-10, SNT-15 and SNT-16 cell lines were treated with the respective concentrations of an inhibitor of EZH2 (DZNep), and dimethylsulfoxide (DMSO) (0.1%) treated cell lines served as vehicle controls. Treated cells were diluted in phosphate buffered saline (PBS), sonicated and then pelleted by centrifugation at 300g for 5 min. The cell pellet was then resuspended in lysis buffer with a cocktail of protease inhibitors (Promega, Madison, WI). Protein detection by Western blot was done to confirm the expression of EZH2 protein after treatment with DZNep by electrophoretic transfer of equal amounts of sodium dodecyl sulfate-polyacrylamide gel electrophoresis (SDS-PAGE) separated proteins to polyvinylidene fluoride (PVDF) membranes (Bio-Rad, Hercules, CA), then incubation with the respective primary antibodies: EZH2 (Cell Signaling Tech. Inc., Danvers, MA) and β-actin control (Santa Cruz, Dallas, TX), followed by exposure to horseradish peroxidase (HRP)-conjugated secondary antibodies (Santa Cruz) and detection using chemiluminescence (GE Healthcare, Uppsala, Sweden).

Apoptotic cell death analyses were carried out following DZNep treatment using Annexin-V-allophycocyanin (APC) and propidium iodide (PI) detection systems. Following treatment of cells with respective concentrations of DZNep and DMSO (0.1%) as vehicle controls and incubation for 72 h, the cells were collected and washed in PBS. The staining of apoptotic cells by Annexin-V-APC was assayed using an APC Annexin-V Apoptosis Detection Kit (BD Pharmingen, San Jose, CA) according to the

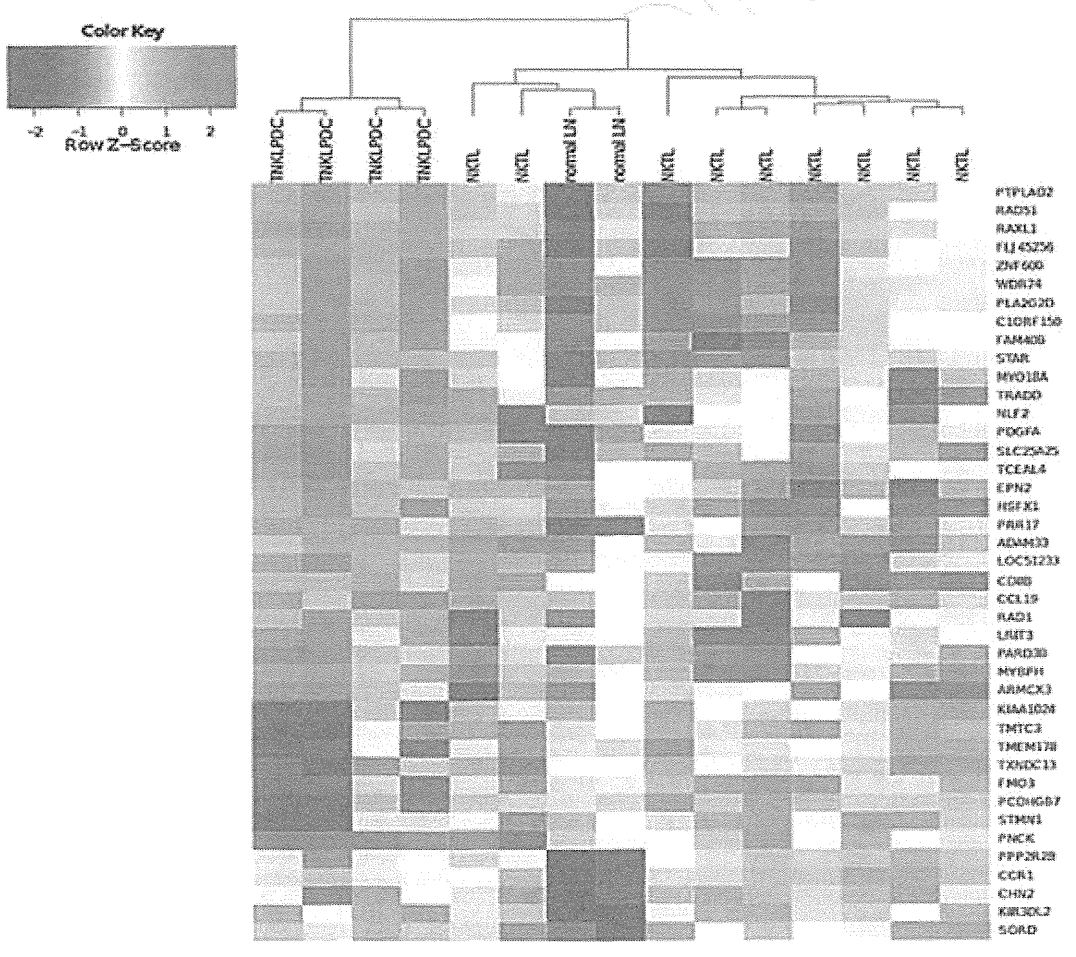

Figure 1. Heatmap showing differentially expressed genes between EBV-associated T/NK lymphoproliferative disorder in children (TNKLPDC) and nasal-type NK/T-cell lymphoma (NKTL). normal LN, normal lymph node.

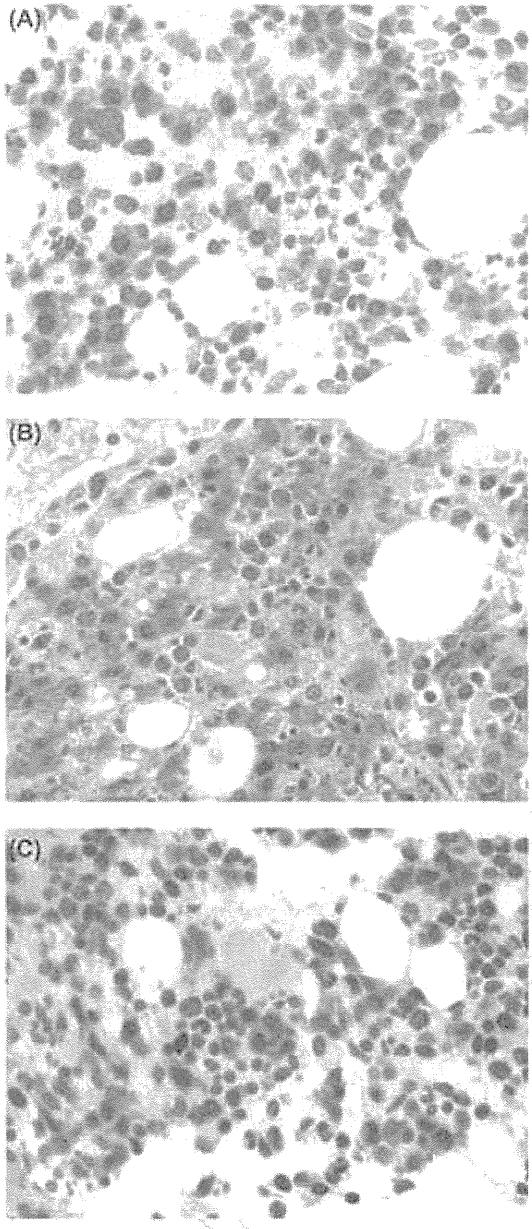

Figure 2. Overexpression of EZH2, p53 and survivin in cases of TNKLPDC. Immunohistochemistry reveals overexpression of EZH2 in case 19 (A, EZH2/CD3 double stain, EZH2 stains nucleus brown and CD3 stains cell membrane/cytoplasm red, original magnification × 600), p53 in case 15 (B, p53/CD3 double stain, p53 stains nucleus brown and CD3 stains cell membrane/cytoplasm red, original magnification × 600) and survivin in case 18 (C, survivin/CD3 double stain, survivin stains nucleus brown and CD3 stains cell membrane/cytoplasm red, original magnification × 600). All photographs were taken with a DP20 Olympus camera (Olympus, Tokyo, Japan) using an Olympus BX41 microscope (Olympus). Images were acquired using a DP Controller 2002 (Olympus) and processed using Adobe Photoshop version 5.5 (Adobe Systems, San Jose, CA).

manufacturer's instructions, and the analysis was performed on a BD LSR II (Becton Dickinson) flow cytometer, using BD FACSDiva™ software.

Results

Gene expression profiling revealed a similar molecular signature between NKTL and TNKLPDC with up-regulation of p53, survivin and EZH2 in TNKLPDC

We performed GEP on four cases of TNKLPDC and compared it to the signature of NKTL that we obtained in our previous study. The expression fold-change for each gene between TNKLPDC versus normal and the expression fold-change of each gene between NKTL versus normal (obtained from our previous study) [10] showed a significant correlation, with Pearson correlation coefficient $r = 0.692$, $p < 2.2 \times 10^{-16}$, indicating a high degree of similarity between TNKLPDC and NKTL (Supplementary Figure 1 to be found online at http://informahealthcare.com/doi/abs/10.3109/10428194.2014.983099). Only a small number of genes were significantly differentially expressed between TNKLPDC and NKTL. There were 41 genes showing two-fold or greater difference in expression between TNKLPDC and NKTL, of which 28 were up-regulated and 13 were down-regulated in TNKLPDC compared to NKTL (Figure 1).

Since TNKLPDC shares a similar signature with NKTL at the molecular level, we investigated whether a few of the oncoproteins (p53, survivin and EZH2), which were identified by us to be up-regulated in NKTL in our previous study, are similarly up-regulated in TNKLPDC [10,14]. Indeed, using IHC double stains for p53/CD3, survivin/CD3 and EZH2/CD3, we also found overexpression of p53, survivin and EZH2 in 69% (11/16 cases), 63% (10/16 cases) and 65% (13/20 cases) of our cases of TNKLPDC, respectively, supporting that NKTL and TNKLPDC share similar phenotypic and molecular signatures and hence indirectly validating our GEP results (Figure 2) (Supplementary Table V to be found online at http://informahealthcare.com/doi/abs/10.3109/10428194.2014.983099 for IHC results for p53, survivin and EZH2).

Inhibition of EZH2 by DZNep induced growth inhibition and apoptosis of TNKLPDC cell lines

We previously reported the overexpression of EZH2 in NKTL, and depletion of EZH2 using a PRC2 inhibitor, DZNep, significantly inhibited the growth of NK tumor cells [14]. Hence, we also treated the TNKLPDC cell lines with DZNep [15,16]. Our results demonstrated that DZNep effectively and dose dependently reduced protein levels of EZH2 in KAI-3, SNK-10, SNT-15 and SNT-16 cell lines [Figure 3(A)], resulting in reduction of cell viability [Figure 3(B)] and an increase in apoptosis as detected by Annexin-V analysis using flow cytometry, in a dose-dependent manner [Figure 3(C)] (Supplementary Figure 2 to be found online at http://informahealthcare.com/doi/abs/10.3109/10428194.2014.983099 shows increased apoptosis following DZNep treatment).

TNKLPDC is enriched for gene sets associated with hematopoietic and leukemic stem cells compared to NKTL

Despite the similarity of the molecular signature between TNKLPDC and NKTL, we investigated whether there are subtle differences between them. To achieve this, we performed gene set enrichment analysis (GSEA). Using a

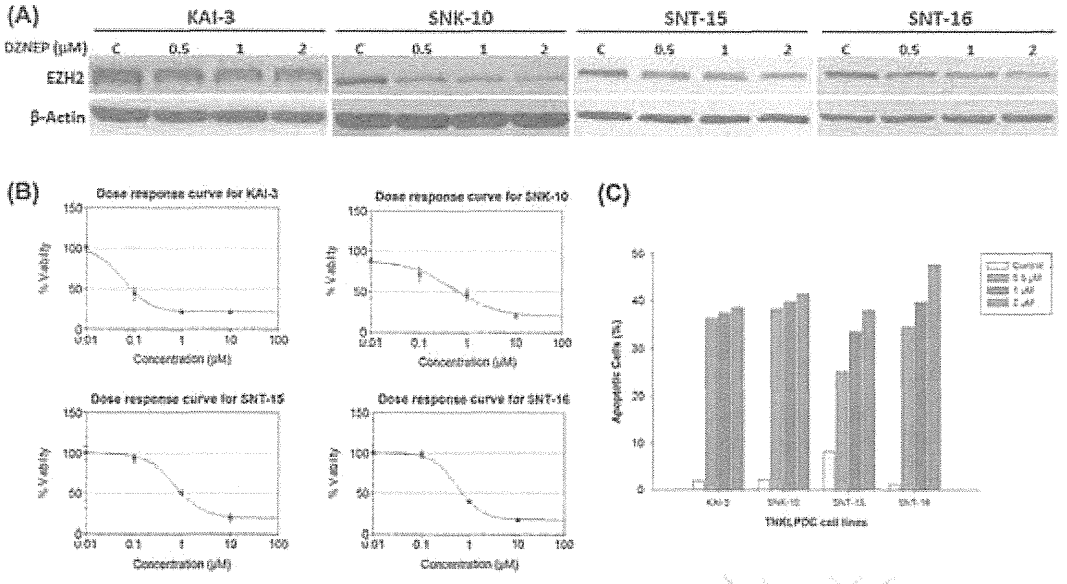

Figure 3. Treatment with DZNep results in a dose-dependent decrease in cellular protein levels of EZH2 in KAI-3, SNK-10, SNT-15 and SNT-16 cell lines (A) and a corresponding reduction in cell viability (B) and increase in apoptosis (C) as detected by flow cytometry.

cut-off false discovery rate of $< 20\%$, we identified 17 gene sets enriched in genes down-regulated in TNKLPDC compared to NKTL (negative enrichment score). Amongst the 17 gene sets, several gene sets of genes down-regulated in stem cells were negatively enriched in TNKLPDC compared to NKTL, meaning that genes down-regulated in stem cells are also down-regulated in TNKLPDC compared to NKTL. This suggests that TNKLPDC shares some molecular feature with stem cells. On the other hand, gene sets of genes up-regulated in invasive/advanced malignancies were negatively enriched in TNKLPDC compared to NKTL, meaning that they are also up-regulated in NKTL compared to TNKLPDC. In other words, NKTL shows up-regulation of genes in invasive tumors and hence shares molecular features with invasive/advanced cancers (Table I) compared to TNKLPDC (Supplementary Figure 3 to be found online at http://informahealthcare.com/doi/abs/10.3109/10428194.2014.983099 shows GSEA enrichment plots of gene sets related to stem cell and invasive/advanced cancers which are negatively enriched in TNKLPDC compared to NKTL). This result is consistent with the different clinical presentation of the two malignancies, with TNKLPDC having a leukemic presentation characterized by bone marrow involvement and cytopenias, and NKTL, in contrast, manifesting mostly as aggressive solid cancers.

To further verify that TNKLPDC may have a more stem cell related phenotype based on the GSEA results, we performed ALDH1 assay in six NKTL cell lines (NK-YS, NK-92, HANK-1, SNK-1, SNK-6, SNT-8) and five TNKLPDC cell lines (KAI-3, SNK-10, SNT-13, SNT-15, SNT-16). ALDH enzymes are a family of intracellular enzymes that participate in cellular detoxification, differentiation and drug resistance through the oxidation of cellular aldehydes [17]. ALDH1-positive cell populations are capable of generating tumor xenografts [18], and ALDH1 is used as a marker of cancer stem cells (CSCs) [19]. The proportion of ALDH1-positive cells in both TNKLPDC and NKTL cell lines ranged from 0.2% to 10.2%, in line with reports that leukemic stem cells constitute only a subfraction of the blast cell population [20,21]. In agreement with the GESA result, there was a significant difference in ALDH1 expression in TNKLPDC compared to NKTL cell lines, with median of 8.15% of cells expressing ALDH1 in TNKLPDC compared to 2.4% in NKTL ($p = 0.04$), suggesting that there was a higher proportion of tumor cells with CSC properties in TNKLPDC compared to NKTL [Figures 4(A) and 4(B)]. Interestingly, the SNK-1 cell line, derived from a 24-year-old patient with TNKLPDC (CAEBV) who subsequently developed NKTL, also demonstrated a higher level of ALDH1 expression compared to cell lines derived from patients with NKTL without a history of TNKLPDC.

Discussion

TNKLPDC is a group of poorly understood lymphoproliferative disorders in children and young adults, which can be difficult to distinguish from the disseminated form of NKTL. The pathobiology is poorly characterized, and the disease is often aggressive with no effective treatment. Various therapies have been tried for the treatment of CAEBV, including antiviral, chemotherapeutic and immunomodulatory drugs, with only limited success. These regimens are not effective in achieving sustainable complete remission, and hematopoietic stem cell transplant (HSCT) seems to be the only curative therapy for CAEBV at present [8].

We report, for the first time, that TNKLPDC shows a similar molecular signature to NKTL. Furthermore, a number of oncoproteins that we have previously shown to be overexpressed in NKTL, such as p53, EZH2 and survivin, are similarly overexpressed in TNKLPDC. This is not unexpected, as both entities are characterized by an

Table I. Gene sets differentially enriched between TNKLPDC and NKTL showing 17 gene sets that are negatively enriched in TNKLPDC compared to NKTL.

Name	Description	Size of gene sets	Enrichment score	FDR *q*-value
VECCHI_GASTRIC_CANCER_ADVANCED_VS_EARLY_UP*	Up-regulated genes distinguishing between two subtypes of gastric cancer: advanced (AGC) and early (EGC)	19	−0.7683091	0
GAL_LEUKEMIC_STEM_CELL_DN†	Genes down-regulated in leukemic stem cells (LSCs), defined as CD34 + CD38− [Gene ID = 947, 952] cells from patients with AML (acute myeloid leukemia) compared to CD34 + CD38+ cells	61	−0.5313042	0.00122956
LU_TUMOR_VASCULATURE_UP	Genes up-regulated in endothelial cells derived from invasive ovarian cancer tissue	6	−0.927103	0.05146535
RUIZ_TNC_TARGETS_DN	Genes down-regulated in T98G cells (glioblastoma) by TNC [Gene ID = 3371].	26	−0.5973733	0.05591349
DAVICIONI_TARGETS_OF_PAX_FOXO1_FUSIONS_DN	Genes down-regulated in RD cells (embryonal rhabdomyosarcoma, ERMS) by expression of PAX3- or PAX7-FOXO1 [Gene ID = 5077, 5081, 2308] fusions off retroviral vectors	10	−0.7663204	0.05456302
POOLA_INVASIVE_BREAST_CANCER_UP*	Genes up-regulated in atypical ductal hyperplastic tissues from patients with (ADHC) breast cancer vs. those without the cancer (ADH)	62	−0.4721814	0.08633608
JAATINEN_HEMATOPOIETIC_STEM_CELL_DN†	Genes down-regulated in CD133+ [Gene ID = 8842] cells (hematopoietic stem cells, HSCs) compared to CD133 − cells	56	−0.4827268	0.07452668
TURASHVILI_BREAST_LOBULAR_CARCINOMA_VS_LOBULAR_NORMAL_UP*	Genes up-regulated in lobular carcinoma vs. normal lobular breast cells.	13	−0.6917861	0.09243327
SCHUETZ_BREAST_CANCER_DUCTAL_INVASIVE_UP*	Genes up-regulated in invasive ductal carcinoma (IDC) relative to ductal carcinoma *in situ* (DCIS, non-invasive)	58	−0.4718207	0.08723507
AKL_HTLV1_INFECTION_DN	Genes down-regulated in WE17/10 cells (CD4+ [Gene ID = 920] T lymphocytes) infected by HTLV1 (and thus displaying low CD7 [Gene ID = 924]) compared to uninfected (i.e. CD7+) cells	10	−0.7377943	0.12973607
SANA_RESPONSE_TO_IFNG_DN	Genes down-regulated in five primary endothelial cell types (lung, aortic, iliac, dermal,and colon) by IFNG [Gene ID = 3458].	10	−0.7334317	0.11817111
LEE_LIVER_CANCER_MYC_E2F1_UP	Genes up-regulated in hepatocellular carcinoma (HCC) from MYC and E2F1 [Gene ID = 4609, 1869] double transgenic mice	14	−0.6603344	0.12351392
TAKEDA_TARGETS_OF_NUP98_HOXA9_FUSION_3D_DN†	Genes down-regulated in CD34+ [Gene ID = 947] hematopoetic cells by expression of NUP98-HOXA9 fusion [Gene ID = 4928, 3205] off a retroviral vector at 3 days after transduction	9	−0.7459078	0.13656901
VERHAAK_AML_WITH_NPM1_MUTATED_UP	Genes up-regulated in patients with acute myeloid leukemia (AML) with mutated NPM1 [Gene ID = 4869]	58	−0.452349	0.13712986
MCCLUNG_CREB1_TARGETS_DN	Genes down-regulated in the nucleus accumbens (a major reward center in the brain) 8 weeks after induction of CREB1 [Gene ID = 1385] expression in a transgenic Tet-Off system	6	−0.848532	0.15731472
SMID_BREAST_CANCER_RELAPSE_IN_BONE_UP*	Genes up-regulated in bone relapse of breast cancer	16	−0.6191868	0.1730245
MCLACHLAN_DENTAL_CARIES_DN	Genes down-regulated in pulpal tissue extracted from carious teeth	57	−0.4333106	0.17132571

TNKLPDC, Epstein-Barr virus-associated T/natural killer-cell lymphoproliferative disorder in children and young adults; NKTL, extranodal nasal natural killer/T-cell lymphoma; FDR, false discovery rate.
*Gene sets of genes up-regulated in invasive/advanced malignancies.
†Gene sets of genes down-regulated in stem cells.

EBV-associated cytotoxic T/NK proliferation and share similar clinical features.

Despite the similarity, there are some subtle differences in the molecular profile. Our GESA data revealed a distinctive enrichment of stem cell related genes in TNKLPDC compared to NKTL. Indeed, the expression of ALDH1, a marker of stem cell properties, was significantly higher in TNKLPDC compared to NKTL cell lines, and this supports the validity of our GESA result. On the other hand, genes overexpressed in advanced malignancies were enriched in NKTL. This result is consistent with the different clinical presentation of the two malignancies, with TNKLPDC having a leukemic presentation characterized by bone marrow involvement and cytopenias, and NKTL, in contrast, manifesting as aggressive solid cancers.

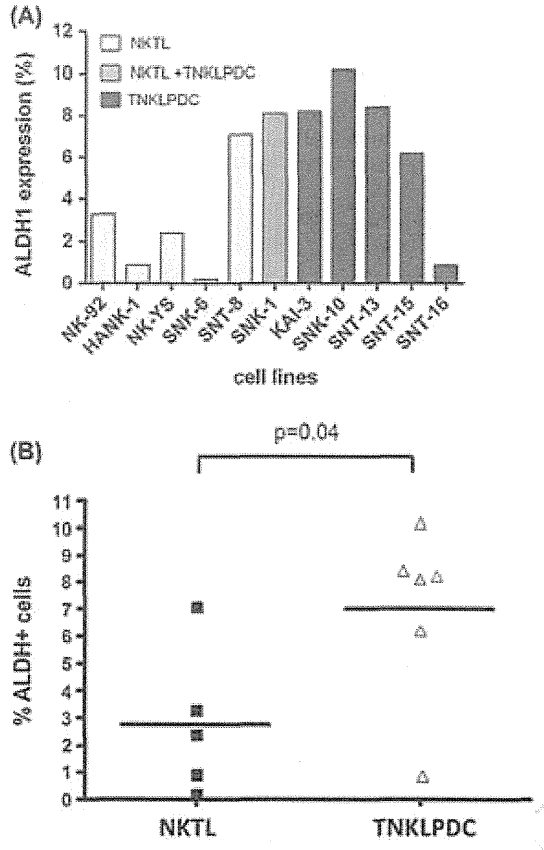

Figure 4. (A) TNKLPDC cell lines show a higher proportion of cells expressing ALDH1 compared to NKTL cell lines. (B) TNKLPDC cell lines show a significantly higher proportion of cells expressing ALDH1 compared to NKTL cell lines (median expression of 8.15% vs. 2.4%, $p = 0.04$).

The CSC hypothesis proposes that tumors arise from a subset of cells (usually representing the minority population) with distinctive stem cell properties characterized by the ability to undergo self-renewal, proliferation and multipotential differentiation [22,23]. A role for CSCs has been characterized for acute leukemias [24], and CSCs also exist in solid tumors, including brain, breast and colon [25]. In acute myeloid leukemia, only a subfraction of cells are proposed to be leukemia stem cells (LSCs), while the majority of cells are either transitional cells with limited proliferative capacity or more differentiated end cells [21]. In general, these CSCs are quiescent and resistant to conventional chemotherapy that usually targets proliferating cells. Hence, our discovery of potential CSC properties in TNKLPDC cell lines has important therapeutic implications in this group of disorders. In addition, this may also explain the success of allogeneic HSCT in the treatment of TNKLPDC [26–28] and why conventional chemotherapy, without HSCT, is often unsuccessful in the treatment of TNKLPDC.

Although HSCT at present appears to be curative for patients with CAEBV, it is not without life-threatening complications. In this regard, identification of new therapeutic strategies and targets is greatly needed. Importantly, we demonstrated EZH2 to be aberrantly overexpressed in TNKLPDC. EZH2 is a H3K27-specific histone methyltransferase and a component of the polycomb repressive complex 2 (PRC2), which plays a key role in the epigenetic maintenance of the repressive chromatin mark and has been implicated to play an oncogenic role in cancers [29]. Our *in vitro* studies using DZNep, a compound capable of inhibiting EZH2 by depleting PRC2 components [15], showed that successful down-regulation of EZH2 in four TNKLPDC cell lines led to a significant increase in apoptosis and decrease in the viability of tumor cells. Although DZNep is not a specific inhibitor of EZH2 and may affect other molecules [30], our results suggest that EZH2 may be important for survival of TNKLPDC cells, and down-regulation/degradation of EZH2 could be a potential therapeutic strategy in TNKLPDC. This is of interest, as EZH2 inhibitors are currently being developed for clinical use [31,32].

In conclusion, our study showed that the molecular and phenotypic signature of TNKLPDC is similar to NKTL, with overexpression of p53, survivin and EZH2. Down-regulation of EZH2 results in an increase in apoptosis and reduction in cell viability, supporting the rationale for targeting EZH2 as a potential therapeutic strategy in the treatment of NKTL. In addition, the novel discovery of potential CSC properties in TNKLPDC cell lines has important therapeutic implications in this group of disorders, although this finding requires further validation in primary tumor samples in a larger cohort of patients.

Acknowledgements

S.-B.N. is supported by a National University Health System Clinician Scientist Program award. This work was partially supported by a grant from the Ministry of Education (MOE) Academic Research Fund (AcRF) Tier 1 (WBS No. R-179-000-046-112).

W.-J.C. is supported by a NMRC Clinician Scientist Investigator award. This work was partially supported by a Singapore Cancer Syndicate Grant, and the National Research Foundation Singapore and Singapore Ministry of Education under the Research Centers of Excellence initiative.

Potential conflict of interest: Disclosure forms provided by the authors are available with the full text of this article at www.informahealthcare.com/lal.

References

[1] Quintanilla-Martinez L, Kimura H, Jaffe ES. EBV-positive T-cell lymphoproliferative disorders of childhood. In: Swerdlow SH, Campo E, Harris NL, et al., editors. WHO classification of tumours of haematopoietic and lymphoid tissues. 4th ed. Lyon: IRAC Press; 2008. pp 278–280.

[2] Ko YH, Jaffe ES. Epstein-Barr virus-positive systemic T-lymphoproliferative disorders and related lymphoproliferations of childhood. In: Jaffe ES, Harris NL, Vardiman JW, et al., editors. Hematopathology. Philadelphia, PA: Elsevier Saunders; 2011. pp 492–505.

[3] Cohen JI, Kimura H, Nakamura S, et al. Epstein-Barr virus-associated lymphoproliferative disease in non-immunocompromised hosts: a status report and summary of an international meeting, 8–9 September 2008. Ann Oncol 2009;20:1472–1482.

[4] Kimura H, Ito Y, Kawabe S, et al. EBV-associated T/NK-cell lymphoproliferative diseases in nonimmunocompromised hosts: prospective analysis of 108 cases. Blood 2012;119:673–686.
[5] Ohshima K, Kimura H, Yoshino T, et al. Proposed categorization of pathological states of EBV-associated T/natural killer-cell lymphoproliferative disorder (LPD) in children and young adults: overlap with chronic active EBV infection and infantile fulminant EBV T-LPD. Pathol Int 2008;58:209–217.
[6] Wang RC, Chang ST, Hsieh YC, et al. Spectrum of Epstein-Barr virus-associated T-cell lymphoproliferative disorder in adolescents and young adults in Taiwan. Int J Clin Exp Pathol 2014;7:2430–2437.
[7] Hong M, Ko YH, Yoo KH, et al. EBV-positive T/NK-cell lymphoproliferative disease of childhood. Korean J Pathol 2013;47: 137–147.
[8] Fujiwara S, Kimura H, Imadome K, et al. Current research on chronic active Epstein-Barr virus infection in Japan. Pediatr Int 2014;56:159–166.
[9] Isobe Y, Aritaka N, Setoguchi Y, et al. T/NK cell type chronic active Epstein-Barr virus disease in adults: an underlying condition for Epstein-Barr virus-associated T/NK-cell lymphoma. J Clin Pathol 2012;65:278–282.
[10] Ng SB, Selvarajan V, Huang G, et al. Activated oncogenic pathways and therapeutic targets in extranodal nasal-type NK/T cell lymphoma revealed by gene expression profiling. J Pathol 2010;223: 496–510.
[11] Fan JB, Yeakley JM, Bibikova M, et al. A versatile assay for high-throughput gene expression profiling on universal array matrices. Genome Res 2004;14:878–885.
[12] Bibikova M, Talantov D, Chudin E, et al. Quantitative gene expression profiling in formalin-fixed, paraffin-embedded tissues using universal bead arrays. Am J Pathol 2004;165:1799–1807.
[13] Tusher VG, Tibshirani R, Chu G. Significance analysis of microarrays applied to the ionizing radiation response. Proc Natl Acad Sci USA 2001;98:5116–5121.
[14] Yan J, Ng SB, Tay JL, et al. EZH2 overexpression in natural killer/T-cell lymphoma confers growth advantage independently of histone methyltransferase activity. Blood 2013;121:4512–4520.
[15] Tan J, Yang X, Zhuang L, et al. Pharmacologic disruption of Polycomb-repressive complex 2-mediated gene repression selectively induces apoptosis in cancer cells. Genes Dev 2007;21:1050–1063.
[16] Xie Z, Bi C, Cheong LL, et al. Determinants of sensitivity to DZNep induced apoptosis in multiple myeloma cells. PLoS One 2011;6:e21583.
[17] Moreb J, Schweder M, Suresh A, et al. Overexpression of the human aldehyde dehydrogenase class I results in increased resistance to 4-hydroperoxycyclophosphamide. Cancer Gene Ther 1996;3:24–30.
[18] Huang EH, Hynes MJ, Zhang T, et al. Aldehyde dehydrogenase 1 is a marker for normal and malignant human colonic stem cells (SC) and tracks SC overpopulation during colon tumorigenesis. Cancer Res 2009;69:3382–3389.
[19] Liang D, Shi Y. Aldehyde dehydrogenase-1 is a specific marker for stem cells in human lung adenocarcinoma. Med Oncol 2012;29: 633–639.
[20] Hwang K, Park CJ, Jang S, et al. Flow cytometric quantification and immunophenotyping of leukemic stem cells in acute myeloid leukemia. Ann Hematol 2012;91:1541–1546.
[21] Kummermehr JC. Tumour stem cells—the evidence and the ambiguity. Acta Oncol 2001;40:981–988.
[22] Dick JE. Stem cell concepts renew cancer research. Blood 2008;112:4793–4807.
[23] Jordan CT. Cancer stem cell biology: from leukemia to solid tumors. Curr Opin Cell Biol 2004;16:708–712.
[24] Hope KJ, Jin L, Dick JE. Human acute myeloid leukemia stem cells. Arch Med Res 2003;34:507–514.
[25] Ailles LE, Weissman IL. Cancer stem cells in solid tumors. Curr Opin Biotechnol 2007;18:460–466.
[26] Gotoh K, Ito Y, Shibata-Watanabe Y, et al. Clinical and virological characteristics of 15 patients with chronic active Epstein-Barr virus infection treated with hematopoietic stem cell transplantation. Clin Infect Dis 2008;46:1525–1534.
[27] Sato E, Ohga S, Kuroda H, et al. Allogeneic hematopoietic stem cell transplantation for Epstein-Barr virus-associated T/natural killer-cell lymphoproliferative disease in Japan. Am J Hematol 2008; 83:721–727.
[28] Kawa K, Sawada A, Sato M, et al. Excellent outcome of allogeneic hematopoietic SCT with reduced-intensity conditioning for the treatment of chronic active EBV infection. Bone Marrow Transplant 2011;46:77–83.
[29] Chang CJ, Hung MC. The role of EZH2 in tumour progression. Br J Cancer 2012;106:243–247.
[30] Miranda TB, Cortez CC, Yoo CB, et al. DZNep is a global histone methylation inhibitor that reactivates developmental genes not silenced by DNA methylation. Mol Cancer Ther 2009;8:1579–1588.
[31] McCabe MT, Ott HM, Ganji G, et al. EZH2 inhibition as a therapeutic strategy for lymphoma with EZH2-activating mutations. Nature 2012;492:108–112.
[32] Knutson SK, Wigle TJ, Warholic NM, et al. A selective inhibitor of EZH2 blocks H3K27 methylation and kills mutant lymphoma cells. Nat Chem Biol 2012;8:890–896.

Supplementary material available online

Supplementary Tables I–V and Figures 1–3 showing further data.

OPEN ACCESS Freely available online

PLOS | ONE

CD137 Expression Is Induced by Epstein-Barr Virus Infection through LMP1 in T or NK Cells and Mediates Survival Promoting Signals

Mayumi Yoshimori[1,2], Ken-Ichi Imadome[3], Honami Komatsu[1,2], Ludan Wang[1], Yasunori Saitoh[4], Shoji Yamaoka[4], Tetsuya Fukuda[1], Morito Kurata[5], Takatoshi Koyama[2], Norio Shimizu[6], Shigeyoshi Fujiwara[3], Osamu Miura[1], Ayako Arai[1]*

1 Department of Hematology, Graduate School of Medical and Dental Sciences, Tokyo Medical and Dental University, Tokyo, Japan, **2** Department of Laboratory Molecular Genetics of Hematology, Graduate School of Health Care Sciences, Tokyo Medical and Dental University, Tokyo, Japan, **3** Department of Infectious Diseases, National Research Institute for Child Health and Development, Tokyo, Japan, **4** Department of Molecular Virology, Graduate School of Medical and Dental Sciences, Tokyo Medical and Dental University, Tokyo, Japan, **5** Department of Comprehensive Pathology, Graduate School of Medical and Dental Sciences, Tokyo Medical and Dental University, Tokyo, Japan, **6** Department of Virology, Division of Medical Science, Medical Research Institute, Tokyo Medical and Dental University, Tokyo, Japan

Abstract

To clarify the mechanism for development of Epstein-Barr virus (EBV)-positive T- or NK-cell neoplasms, we focused on the costimulatory receptor CD137. We detected high expression of *CD137* gene and its protein on EBV-positive T- or NK-cell lines as compared with EBV-negative cell lines. EBV-positive cells from EBV-positive T- or NK-cell lymphoproliferative disorders (EBV-T/NK-LPDs) patients also had significantly higher *CD137* gene expression than control cells from healthy donors. In the presence of IL-2, whose concentration in the serum of EBV-T/NK-LPDs was higher than that of healthy donors, CD137 protein expression was upregulated in the patients' cells whereas not in control cells from healthy donors. *In vitro* EBV infection of MOLT4 cells resulted in induction of endogenous CD137 expression. Transient expression of *LMP1*, which was enhanced by IL-2 in EBV-T/NK-LPDs cells, induced endogenous *CD137* gene expression in T and NK-cell lines. In order to examine *in vivo* CD137 expression, we used EBV-T/NK-LPDs xenograft models generated by intravenous injection of patients' cells. We identified EBV-positive and CD8-positive T cells, as well as CD137 ligand-positive cells, in their tissue lesions. In addition, we detected CD137 expression on the EBV infected cells from the lesions of the models by immune-fluorescent staining. Finally, CD137 stimulation suppressed etoposide-induced cell death not only in the EBV-positive T- or NK-cell lines, but also in the patients' cells. These results indicate that upregulation of CD137 expression through LMP1 by EBV promotes cell survival in T or NK cells leading to development of EBV-positive T/NK-cell neoplasms.

Citation: Yoshimori M, Imadome K-I, Komatsu H, Wang L, Saitoh Y, et al. (2014) CD137 Expression Is Induced by Epstein-Barr Virus Infection through LMP1 in T or NK Cells and Mediates Survival Promoting Signals. PLoS ONE 9(11): e112564. doi:10.1371/journal.pone.0112564

Editor: Joseph S. Pagano, The University of North Carolina at Chapel Hill, United States of America

Received April 22, 2014; **Accepted** October 20, 2014; **Published** November 19, 2014

Funding: This work was supported by a grant from the Ministry of Health, Labor, and Welfare of Japan (H22-Nanchi-080) as well as a grant from the Ministry of Education, Culture, Sports, Science, and Technology of Japan (23591375). The funders had no role in study design, data collection and analysis, decision to publish, or preparation of the manuscript.

Competing Interests: The authors have declared that no competing interests exist.

* Email: ara.hema@tmd.ac.jp

Introduction

Epstein-Barr virus (EBV) infection can be found in lymphoid malignancies not only of B-cell lineage, but also of T- or NK-cell lineages. These EBV-positive T or NK-cell neoplasms, such as extranodal NK/T-cell lymphoma nasal type (ENKL), aggressive NK-cell leukemia (ANKL), and EBV-positive T- or NK- cell lymphoproliferative diseases (EBV-T/NK-LPDs), are relatively rare but lethal disorders classified as peripheral T/NK-cell lymphomas according to the WHO classification of tumors of hematopoietic and lymphoid malignancies. ENKL is a rapidly progressive lymphoma characterized by extranodal lesions with vascular damage and severe necrosis accompanied by infiltration of neoplastic NK or cytotoxic T cells [1]. ANKL is a markedly aggressive leukemia with neoplastic proliferation of NK cells [2]. EBV-T/NK-LPDs is a fatal disorder presenting sustained infectious mononucleosis-like symptoms, hypersensitivity to mosquito bites, or hydroa vacciniforme-like eruption accompanied by clonal proliferation of EBV-infected cells [3,4]. Because most reported cases were children or young adults, and were mainly of the T-cell-infected type, the disorders were designated "EBV-positive T-cell lymphoproliferative diseases of childhood" in the WHO classification, although adult and NK-cell types have been reported [4–6]. The common clinical properties of EBV-T/NK-neoplasms are the presence of severe inflammation, resistance to chemotherapy, and a marked geographic bias for East Asia and Latin America, suggesting a genetic context for disease development [4]. Since these EBV-T/NK-neoplasms overlap [4], common mechanisms are thought to exist in the background and contribute to disease development.

It is well known that EBV infects B cells and makes the infected cells immortal resulting in B-cell lymphomas. Similarly it is suspected that EBV may also cause T- or NK-cell neoplasms. However, why and how EBV latently infects T or NK cells,

whether or not EBV directly causes these malignancies, and the mechanism of action responsible for the disease development remain to be clarified. Although new chemotherapy and stem cell transplantation have achieved good results for EBV-T/NK neoplasms recently [7–9], prognosis of the diseases is still poor. The mechanisms for development of the disease need to be determined to establish an optimal treatment.

To clarify the molecular mechanism underlying the development of EBV-T/NK-neoplasms, we focused on the costimulatory receptor CD137. CD137, also known as 4-1BB, is a member of the tumor necrosis factor (TNF) receptor superfamily, and expressed on the surface of activated T and NK cells [10]. In association with TCR stimulation, it plays a pivotal role in proliferation, survival, and differentiation of these cells as a costimulatory molecule [11]. Recently, it was reported that CD137 is expressed on tumor cells from adult T-cell leukemia/lymphoma (ATLL) and from T-cell lymphomas [12,13]. Here we found CD137 expression on EBV-positive cells in EBV-T/NK-neoplasms and investigated its role for the lymphomagenesis using established cell lines as well as cells from EBV-T/NK-LPDs patients.

Results

CD137 expression in EBV-T/NK-cell lines

Six EBV-positive T- and NK-cell lines, SNT8, SNT15, SNT16, SNK1, SNK6, and SNK10 had been established from primary lesions of ENKL patients (SNT8 and SNK6) and PB of EBV-T/NK-LPDs patients (SNT15, SNT16, SNK1, and SNK10) [14]. We investigated *CD137* mRNA expression in the cell lines by RT-PCR. *CD137* mRNA was expressed in all of them, whereas EBV-negative T-cell lines (Jurkat, MOLT4, and HPB-ALL) and NK-cell line (KHYG1) were negative for the expression (Figure 1A). The mRNA was detected but weak in an EBV-negative NK-cell line, MTA, and in EBV-negative B-cell lines, BJAB, Ramos, and MD901. We also investigated 3 EBV-positive B cell lines, Raji, a lymphoblastoid cell line (LCL), and HS-sultun. The expression was detected in Raji. The expression was weak in LCL, and negative in HS-Sultan. We next investigated CD137 protein expression on the cell surface. Figure 1B shows that CD137 protein was expressed on the cell surface of all EBV-positive T- or NK-cells. In contrast, EBV-negative T-, NK-, and B-cell lines were negative for CD137 expression. On the basis of these results, we concluded that CD137 expression was induced at the mRNA and protein levels in EBV-T/NK cell lines. The expression was detected in 2 of 3 examined EBV-positive B cell lines, Raji and LCL, whereas negative in HS-Sultan. The expression in EBV-positive B cells was insignificant in comparison with EBV-positive T or NK cells. We were unable to detect CD137L expression on the surface these EBV-positive T- or NK-cells lines. The expression was negative on them (Figure S1).

EBV induces CD137 expression in T and NK cells

To clarify whether EBV could directly induce CD137 expression, we performed *in vitro* EBV infection of an EBV-negative cell line MOLT4. EBV DNA copy number of EBV-infected MOTL4 cells was 8.8×10^5 copies/μgDNA. EBV infection was verified by the presence of EBV nuclear antigen (EBNA) 1 protein expression (Figure 2A). Most cells were positive for EBNA1. The infection was also confirmed by the presence of the viral mRNA, *LMP1* and *EBNA1*, and the absence of *EBNA2* by RT-PCR (Figure 2B). This expression pattern was classified as latency type 2. *CD137* mRNA was also expressed in EBV-infected MOTL4 cells (Figure 2B and 2C). In addition, Figure 2D showed that CD137 protein expression was detected on EBV-infected MOLT4 cells. We therefore concluded that EBV infection induced mRNA and surface protein expression of CD137 in MOLT4 cells.

CD137 expression in cells from EBV-T/NK-LPDs patients

The above results were validated using EBV-T/NK cells derived from patients. In EBV-T/NK-LPDs, EBV infection could be detected in a particular fraction of PBMCs and isolated at high purity using antibody-conjugated magnetic beads as described in "Materials and Methods". Seventeen patients (aged 8–72 years; 7 males, 10 females; 10 T- and 7 NK-cell types; CD4 type $n=4$, CD8 type $n=5$, γδ type $n=1$, and CD56 type $n=7$) were diagnosed with EBV-T/NK-LPDs according to the criteria as described in "Materials and Methods". We determined the EBV-positive fraction of the lymphocytes in the PB at the diagnosis. The phenotype of the infected cells and EBV DNA load of them were presented in Table 1. EBV DNA was negative or relatively low in CD19-positive cell which EBV can infect (Table 1).

To examine CD137 expression in the EBV-positive fraction, the fractions were isolated by the magnetic beads and obtained for *CD137* mRNA detection in 10 patients. Figure 3A shows the *CD137* mRNA levels in the freshly isolated cells of EBV-positive cell fraction in PBMCs of each patient. *CD137* mRNA levels in CD4-, CD8-, and CD56-positive cell fractions of 5 healthy donors' PBMCs were also demonstrated. The mRNA levels in the patients' cells were significantly higher than those in the cells of healthy donors. Next we examined the expression of CD137 protein by flow cytometry. It showed low expression in freshly isolated PBMCs from both patients and 5 healthy donors (data not shown). However, after culture with IL-2 for 3 days, the expression was increased on the surface of PBMCs from 15 patients but still low on the cells isolated from 5 healthy donors (Figure 3B). The average of CD137 protein levels of EBV-T/NK-LPDs patients was significantly higher than that of healthy donors (Figure 3C). Two-color flow cytometry using antibodies to CD137 and to surface proteins expressed on EBV-positive cells could be performed in 7 patients, and a double-staining pattern was observed in them, whereas fractions from a healthy donor barely expressed the CD137 protein. (Figure S2).

EBV LMP1 induces CD137 expression in T and NK cells through LMP1 induced by IL-2

We investigated the mechanism of enhanced-CD137 expression by IL-2. First we performed luciferase reporter assay with a plasmid containing the *CD137* gene promoter. As shown in Figure 2A, EBV-infected MOLT4 cells were shown to express EBV-encoded proteins including LMP1, and EBNA1, considered to be latency type 2. So, MOLT4 cells were cotransfected with expression plasmids capable of expressing either of EBV-encoded proteins, LMP1, LMP2A, LMP2B or EBNA1. As shown in Figure 4A, LMP1 induced significant upregulation of *CD137* promoter activity, whereas the other molecules did not. Furthermore, in a transient expression assay with these viral proteins in MOLT4 cells, transcription of endogenous *CD137* mRNA was detected only in the LMP1-transfected cells (Figure 4B). These results indicated that, among the EBV proteins, LMP1 transactivated *CD137* expression in T and NK cells. Next we examined whether LMP1 expression was enhanced by IL-2 and might contribute to upregulation of CD137 expression in patients' cells. We isolated PBMCs from EBV-T/NK-LPDs patient (CD4-1) and cultured them with or without IL-2. As shown in Figure 4C, semi-quantitative RT-PCR demonstrated that *LMP1* mRNA was increased in IL-2-treated PBMCs. *CD137* mRNA was also increased in the IL-2-treated cells (Figure 4D). To confirm the

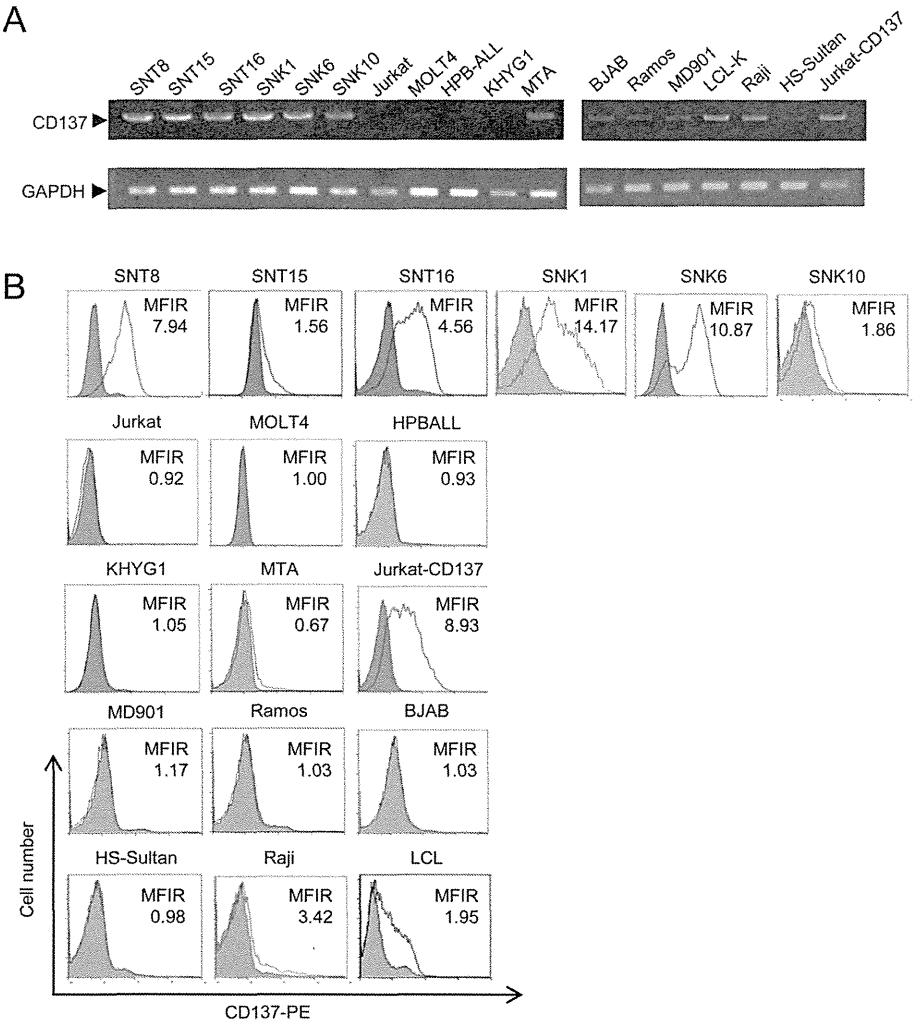

Figure 1. CD137 expression in Epstein-Barr virus (EBV)-positive T- or NK-cell lines. (A) Transcripts of *CD137* (the upper panel) and *GAPDH* (the lower panel) in EBV- positive T- or NK-cell lines were examined by RT-PCR. EBV negative T-, NK, B-cell lines, and EBV-positive B-cell lines were also obtained for the examination. (B) Surface expression of CD137 was examined by flow cytometry using an antibody to CD137 (open histogram) or isotype-matched control immunoglobulin (gray, shaded histogram). The mean fluorescent intensity of CD137 was normalized by that of isotype-matched control and expressed as mean fluorescence intensity rate (MFIR). Each experiment was independently performed more than 3 times and their average data are presented.
doi:10.1371/journal.pone.0112564.g001

in vivo contribution of IL-2 for CD137 expression, we examined the serum concentration of IL-2 in 7 EBV-T/NK-LPDs patients and 5 healthy donors. The concentration in the patients was 0.9-2.4 U/mL in 6 of 7 patients, whereas it was undetectable in 4 of 5 healthy donors (Table 2). These results suggested that CD137 expression was enhanced in the presence of IL-2 most likely through enhanced-expression of LMP1 in EBV-T/NK-LPDs patient cells.

CD137 was detected in EBV-positive cells infiltrating in the tissue lesion of EBV-T/NK-LPDs xenograft model

Next, we examined the CD137 expression on the EBV-positive cells infiltrating into the tissue of EBV-T/NK-LPDs. Since we could not perform the examination for human specimen due to difficulty of obtaining the samples, we used the xenograft models generated by intravenous injection of PBMCs from CD8-3 patient [15]. The injected cells were 2×10^6 in number for each mouse and include CD8-positive EBV-infected cells with clonally proliferation from CD8-3 patient. EBV DNA load of the infected cells were more than 1.0×10^4 copies/μgDNA. After engraftment, which was defined as detection of EBV DNA in the PB of the model, we performed autopsy. Nine mice were examined and the representative data were shown. As shown in Figure 5A–D, infiltration of EBV-positive and CD8-positive cells into the periportal regions in the liver was detected. 79.2% (396/500) of the infiltrating cells were EBER-positive, and 77.4% (387/500) of the cells were CD8-positive. These results indicated that most infiltrating cells were both positive for CD8 and EBER. Although CD137L-positive cells were also detected in the lesion, the number was markedly smaller than that of EBV-positive cells (Figure 5D). In order to determine CD137 expression on EBV-infected cells, we performed immune-fluorescent staining for the infiltrating cells in the lesions. As shown in Figure 5E, EBNA1-positive and CD137-positive cells were detected in the cells isolated from the lesions. LMP1 expression